

“Development and wear analysis of flyash/graphite filled copper alloy composite for bearing application”

**A THESIS SUBMITTED IN PARTIAL FULFILLMENT OF THE
REQUIREMENT**

FOR THE AWARD OF THE DEGREE OF

Master of Technology

In

Production Engineering

**Prepared by
Abhishek Pandey
2013PPE5281**



**MECHANICAL ENGG DEPARTMENT
MALAVIYA NATIONAL INSTITUTE OF TECHNOLOGY JAIPUR
June 2015**



MALAVIYA NATIONAL INSTITUTE OF TECHNOLOGY JAIPUR
JAIPUR – 302017 (RAJASTHAN), INDIA

CERTIFICATE

This is to certify that the dissertation entitled “**Development and wear analysis of flyash/graphite filled copper alloy composite for bearing application**” being submitted by **ABHISHEK PANDEY (2013PPE5281)** is a bonafide work carried out by him under my supervision and guidance, and hence approved for submission to the **Department of Mechanical Engineering, Malaviya National Institute of Technology Jaipur** in partial fulfillment of the requirements for the award of the degree of **Master of Technology (M.Tech.) in Production Engineering**. The matter embodied in this dissertation report has not been submitted anywhere else for award of any other degree or diploma.

Dr. Amar Pattnaik
Assistant Professor,
Department of Mechanical Engineering,
MNIT Jaipur
Place: Jaipur

Dated: June 2015



MALAVIYA NATIONAL INSTITUTE OF TECHNOLOGY JAIPUR
JAIPUR – 302017 (RAJASTHAN), INDIA

CANDIDATE'S DECLARATION

I hereby declare that the work which is being presented in this dissertation entitled **“Development and wear analysis of flyash/graphite filled copper alloy composite for bearing application”** in partial fulfillment of the requirements for the award of the degree of **Master of Technology (M.Tech.) in Production Engineering**, and submitted to the **Department of Mechanical Engineering, Malaviya National Institute of Technology Jaipur** is an authentic record of my own work carried out by me during a period of one year from July 2014 to June 2015 under the guidance and supervision of **Dr. Amar Pattnaik** of the Department of Mechanical Engineering, Malaviya National Institute of Technology Jaipur.

The matter presented in this dissertation embodies the results of my own work and has not been submitted anywhere else for award of any other degree or diploma.

Abhishek Pandey
(2013PPE5281)

This is to certify that the above statement made by the candidate is correct to the best of my knowledge.

Dr. Amar Pattnaik
Supervisor

Place: Jaipur

Dated: June 2015

ACKNOWLEDGEMENT

With great delight, I acknowledge my indebted thanks to my guide and mentor **Dr. Amar Pattnaik** who has always been a source of inspiration and encouragement for me. His stimulated guidance and unwavering support always motivated me to reach out for, and achieve higher levels of excellence. This dissertation could not have attained its present form, both in content and presentation without his active interest, direction and help. I am grateful to him for keeping trust in me in all circumstances. I thank him for being big-hearted with any amateurish mistakes of mine.

I sincerely convey my gratitude to Head of Mechanical Engineering Department **Prof Rakesh Jain**, who made me believe in myself and guided me always. I also convey my gratitude to **Dr.H.S.Mali** who always supported me during my m.tech course. I would like to thank **Prof.Amit pancharya** for his support, understanding and encouragement.

I express my sincere gratitude to **Prof. . G. S. Dangayach for** his support and guidance throughout the course of study at MNIT Jaipur. I would also like to thanks all Technical and Non-Technical Staff of the **Mechanical Engg Department, Metallurgical department and Material research centre** of MNIT Jaipur for their support.

I highly acknowledge and duly appreciate the support extended by my seniors, colleagues-friends and juniors for their help & support in accomplishment of this work during my stay at MNIT Jaipur.

Lastly, I sincerely pay homage to Almighty **God, Parents** and other members of my family for their blessings that aid as a source of energy/inspiration for methroughout the period

- **Abhishek Pandey**

ABSTRACT

Metal matrix composites are playing a great role in fulfilling the demands of various industrial applications and also generating a wide interest in research fraternity. Ball bearing is one of the industry in which metal composites are playing a great role in improving their performance and making them capable of withstanding more severe application with long life and better performance. conventional bearing material such as steel are now a day's getting replaced by metal composites because of their high strength, low wear rate and better chemical properties. The properties of metal matrix composites are greatly influenced by the nature of the reinforcement and hence amalgamation of different reinforcement can yield new properties and can increase the scope of utilization of material in different fields. This thesis is mainly directed towards fabrication of metal matrix composite using C93700 alloy as matrix material and varying percentage of flyash and graphite as the reinforcement material. From the experiment it can be concluded that graphite and flyash helps in improving the mechanical and physical properties such as tensile strength, flexural strength, ductility of C93700 alloy matrix. The most significant advantage of the reinforcement is found to be the improvement in sliding wear properties and decrease in coefficient of friction resulting in better lubrication properties of the composite. At last optimization of wear rate is performed considering the various factors such as load. Reinforcement, sliding distance and sliding velocity. From Taguchi Analysis it is observed that load being the most significant factor in influencing the wear rate followed by the reinforcement while sliding distance is the least significant factor in influencing the wear rate of the composite.

Keywords: C93700 alloy; flyash and graphite; Mechanical properties; Optimization of wear rate

Contents

CERTIFICATE	i
CANDIDATE’S DECLARATION	ii
ACKNOWLEDGEMENT	iii
ABSTRACT	iv
LIST OF FIGURES	ix
LIST OF TABLES	xi
Chapter 1: INTRODUCTION.....	1
1.1 Background and motivation.....	1
1.2 Plain Bearings	1
1.3 Bearing Materials	2
1.3.1 Copper-alloys	3
1.3.2 Aluminum-alloys	3
1.4 Inter layer and Overlay	3
1.5 Lubrication.....	4
1.5.1 Boundary lubrication	5
1.5.2 Mixed Lubrication	5
1.5.3 Full-film lubrication.....	5
1.6 Stribeck-curve	7
1.7 Friction and wear of plain bearings.....	8
1.7.1 Surface roughness’s effects.....	8
1.8 Role of composites in today’s era	9
1.8.1 Characteristics of Particulate filled MMCs	10
1.8.2 Advantages of Composites	10
1.9 Thesis Outline	10
Chapter 2: LITERATURE REVIEW	12
2.1 Study of ball bearing failure under various loading condition	12
2.1.1 Wear and Failure of Bearing Surface	13
2.2 Particulate filled metal matrix composites	15

2.3 Effect of filler content on mechanical properties of metal matrix composites	16
2.4 Effect of filler content on sliding wear behavior of metal matrix composites	20
2.6 Research Gaps.....	22
2.7 Objective of the present work.....	22
Chapter summary	23
Chapter 3: METHODS AND METHODOLOGY	24
3.1 Properties of selected materials	24
3.1.1 Matrix Material.....	24
3.1.2 Reinforcing Materials	25
3.2 Fabrication Method	29
3.2.1 Preheating Of Reinforcement	31
3.2.2 Sample Preparation For Performing The Experiment	31
3.3 Physical and Mechanical characterizations	32
3.3.1 Void Content	32
3.3.2 Hardness.....	33
3.3.3 Tensile Test	34
3.3.4 Flexural Test.....	34
3.3.5 Impact strength.....	35
3.4 X-Ray diffraction Analysis (XRD)	36
3.5 SEM (Scanning electron microscopy).....	37
3.6 Sliding Wear Test.....	37
3.7 Process optimization and Taguchi method.....	38
Chapter summary	40
Chapter 4: PHYSICAL AND MECHANICAL CHARECTERIZATION OF COMPOSITES	41
4.1 Effect of dual reinforced alloy composites on void content.....	41
4.1.1 Theoretical and Experimental density of Dual reinforced C93700 composites ...	41
4.2 Effect of C93700 dual reinforced composites on hardness	45
4.3 Effect of C93700 dual reinforced composites on tensile strength	46
4.4 Effect Of fly ash and graphite on the young's modulus of composite material	48

4.5 Effect Of fly ash and graphite on the Compressive strength of composite material	49
4.6 Effect of fly ash and graphite on the Ductility of composite material	51
4.7 Effect of fly ash and graphite on the Flexural Strength of composite material	52
4.8 Effect Of fly ash and graphite on the Impact Strength of composite material	54
4.9 Effect of reinforcement on coefficient of friction under steady force with variation in sliding speed.	55
4.9.1 Effect of reinforcement on coefficient of friction under steady velocity with variation in Load	57
4.10 Effect of reinforcement on Wear loss(mass loss) under steady load with variation in sliding velocity.....	59
4.10.1 Effect of reinforcement on Wear loss(mass loss) under steady velocity with variation in Load	61
Chapter 5: ANALYSIS OF SURFACE MORPHOLOGY OF PARTICULATE FILLED METAL ALLOY COMPOSITES AND OPTIMIZATION OF WEAR RATE USING TAGUCHI ANALYSIS	63
5.1 Surface morphology and wear analysis of particulate filled metal alloy composites	63
5.2 Effect of XRD on different filler content	67
5.2.1 EDS ANALYSIS OF SAMPLES.....	70
5.3 Optimization of wear rate factor by taguchi method	73
5.4. ANOVA for graphite and flyash filled C93700 alloy composites	76
5.5 Factor settings for minimum Wear rate.....	76
Chapter 6: SUMMARY AND CONCLUSIONS	79
6.1 Effect on Void Content with the Addition of Graphite and Flyash particulate in C93700 alloy matrix.....	79
6.2 Effect on Hardness with the Addition of Graphite and Flyash particulate in C93700 alloy matrix.....	79
6.3 Effect on Tensile Strength with the Addition of Graphite and Flyash particulate in C93700 alloy matrix.....	79
6.4 Effect on Impact Strength with the Addition of Graphite and Flyash particulate in C93700 alloy matrix.....	80

6.5 Effect On Ductility with the Addition of Graphite and Flyash particulate in C93700 alloy matrix.....	80
6.6 Effect on Compression Strength with the Addition of Graphite and Flyash particulate in C93700 alloy matrix	80
6.7 Effect on Flexural Strength with the Addition of Graphite and Flyash particulate in C93700 alloy matrix.....	80
6.8 Effect on Coefficient of Friction (μ) with the Addition of Graphite and Flyash particulate in C93700 alloy matrix	81
6.9 Effect on Wear rate with the Addition of Graphite and Flyash particulate in C93700 alloy matrix.....	81
6.10 Scope for future work.....	81
Chapter summery	82
REFERENCES.....	83

LIST OF FIGURES

Figure 1: Different types of bearing used in various machines[3]	2
Figure 2: Stribeck curve [4]	7
Figure 3: Brinelling and fretting wear of bearing.....	14
Figure 4: Images of Flyash Powder.....	27
Figure 5: SEM of Flyash Powder	27
Figure 6: Arrangement of graphite in layer form.....	28
Figure 7: Images of graphite (i) powder form.....	28
Figure 8: SEM of Graphite powder	29
Figure 9: Images of vacuum chamber die casting	30
Figure 10: Furnance for preheating the reinforcement	31
Figure 11: Surface grinding operation.....	31
Figure 12: Plate after Surface Grinding.....	32
Figure 13: Rockwell Principle	33
Figure 14: Rockwell Equipment	33
Figure 15: Electronic Tensometre	34
Figure 16: Universal Testing Machine	35
Figure 17: Charpy Impact Test Equipment.....	36
Figure 18: XRD equipment used to perform the experiment.....	37
Figure 19: SEM equipment used to perform the experiment.....	37
Figure 20: Figure Equipment used to perform sliding wear test (pin on disc Tribometre) 38	
Figure 21: Experimental and Theoretical density of dual reinforced C93700 alloy composite	42
Figure 22 Effect of void content on C93700 Alloy composites.....	43
Figure 23: SEM images of 0wt% dual reinforcement	43
Figure 24: SEM images of 2wt% dual reinforcement	44
Figure 25 :SEM images of 4wt% dual reinforcement	44
Figure 26: SEM images of 6wt% dual reinforcement	44

Figure 27: SEM images of 8wt% dual reinforcement	45
Figure 28: Effect of hardness graphite and flyash filled alloy Composites	46
Figure 29 :Tensile Strength Of C93700 alloy Composite	48
Figure 30 : Youngs' Modulus of C93700 alloy Composite.....	49
Figure 31 : Compressive Strength Of C93700 alloy Composite.....	51
Figure 32: Ductility of C93700 alloy Composite	52
Figure 33: Flexural Strength Of C93700 alloy Composite	54
Figure 34 : Impact Strength Of C93700 alloy Composite	55
Figure 35: Coefficient of friction Of C93700 alloy Composite under steady force with variation in sliding speed	57
Figure 36: coefficient of friction under steady velocity with variation in Load	59
Figure 37 : Wear loss(mass loss) under steady load with variation in sliding velocity	60
Figure 38 : Wear loss(mass loss) under steady velocity with variation in Load.....	62
Figure 39: SEM images of 0wt% dual reinforcement	65
Figure 40: SEM images of 2 wt% dualreinforcement	65
Figure 41: SEM images of 4 wt% dual reinforcement	65
Figure 42: SEM images of 6 wt% dualreinforcement	66
Figure 43: SEM images of 8 wt% dual reinforcement	66
Figure 44 XRD images of different samples of composites	68
Figure 45 EDS of 8% dual Reinforced C93700 alloy matrix	71
Figure 46 EDS of 6% dual Reinforced C93700 alloy matrix	71
Figure 47 EDS of 4% dual Reinforced C93700 alloy matrix	72
Figure 48 EDS of 2% dual Reinforced C93700 alloy matrix	72
Figure 49 EDS of Pure C93700 Alloy	73
Figure 50 Graph Showing the Effect of different factor on wear rate.....	75

LIST OF TABLES

Table 1: Overview of metal matrix composites mechanical properties	17
Table 2: Physical property of C93700 Alloy	24
Table 3: Mechanical property of C93700 Alloy	25
Table 4: Chemical analysis of flyash.....	26
Table 5: Physical Property Of Graphite.....	29
Table 6: Design of fabricated particulate filled C93700 composite.....	30
Table 7: Orthogonal array for L25 experiment	39
Table 8: Theoretical and Experimental density of Dual reinforced C93700 composites .	41
Table 9 Hardness(Rockwell B of C93700 alloy matrix composite.....	46
Table 10 : Tensile Strength Of C93700 alloy Composite.....	47
Table 11 : Youngs' Modulus Of C93700 alloy Composite	48
Table 12: Compressive Strength Of C93700 alloy Composite	50
Table 13 : Ductility of C93700 alloy Composite	52
Table 14 : Flexural Strength Of C93700 alloy Composite	53
Table 15 : Impact Strength Of C93700 alloy Composite	54
Table 16 : coefficient of friction of C93700 alloy Composite under steady force with variation in sliding speed	56
Table 17 : coefficient of friction under steady velocity with variation in Load	58
Table 18 : Wear loss (mass loss) under steady load with variation in sliding velocity	60
Table 19 : Wear loss (mass loss) under steady velocity with variation in Load.....	62
Table 20 : Experimental design using L ₂₅ orthogonal array (Graphite and flyash filled)	73
Table 21.ANOVA table for wear rate (Graphite and Flyash filled).....	76
Table 22: Response Table for Signal to Noise Ratios	77

NOMENCLATURE

λ	<i>film thickness parameter</i>	
<i>HL</i>	<i>Hydrodynamic lubrication</i>	
<i>EHL</i>	<i>Elasto hydrodynamic lubrication</i>	
<i>Z</i>	<i>Shipper number</i>	
<i>H</i>	<i>Hersey number</i>	
η	<i>Dynamic viscosity</i>	<i>Pas</i>
v	<i>velocity</i>	<i>rpm</i>
ν	<i>Kinematic viscosity</i>	m^2/s
p	<i>Contact pressure</i>	<i>Pa</i>
μ	<i>Friction coefficient</i>	
<i>XRD</i>	<i>X-ray Diffraction</i>	
<i>SEM</i>	<i>Scanning Electron Microscopy</i>	
<i>MMCs</i>	<i>Metal Matrix Composite</i>	
<i>PMMCs</i>	<i>Particulate filled Metal matrix Composite</i>	
<i>CMCs</i>	<i>Ceramic Matrix Composite</i>	
<i>OMCs</i>	<i>Organic Matrix Composite</i>	
<i>UTM</i>	<i>Universal Testing Machine</i>	

Chapter 1: INTRODUCTION

1.1 Background and motivation

Ball bearing durability is one of the high priorities for today's automotive and other industries. One option to decrease the failure of bearing is to decrease the frictional losses by using oils and lubricants with lower viscosities but the changes in lubricants will increase the risk of wear and friction, hence further investigations to minimize wear and wear related failures for bearing is necessary. Friction and wear are one of the most costly phenomena of the today's industry, scientist have been doing a lot of research within the field of tribology to prolong component life and reduce the costs. Material has been always a deep area of interest from ancient times. It is always a deep area of interest for researchers to develop new material with advanced properties at low cost The increased risk of wear for lower viscosity lubricants is, as mentioned, related to a decrease in lubricant film thickness. Thus the surface roughness is one of the important factor to be considered while improving the workability of bearing. For lower viscosity oils, it is clear that the surfaces needs to be smoother, the important question is how smooth it must be in order to maintain the same wear life or durability of components. This introduction mainly focus at providing the basic knowledge within the field of tribology and new hybrid material enabling the reader to follow the experimental investigation on the effect of surface roughness for bearing materials on the corresponding Stribeck-curves. Although this thesis is directed towards the development of particulate filled metal matrix composite for bearing material for plain bearings yet it is also pertinent and applicable to other components e.g. gears, structural applications, automobile components, light material application etc.

1.2 Plain Bearings

According to Yongyong, et al. [1] bearings are designed to transmit the force between two surfaces that are in relative motion minimizing the friction while at the same time allowing the component movement [13]



Figure 1: Different types of bearing used in various machines[3]

There are several types of bearings but they are mainly classified under two broad categories i.e., sliding (plain) bearings and rolling element bearings (Figure 1). Plain bearings are further classified as thrust and journal bearing having two surfaces brought into movement and are separated by a lubricant film. Depending on the design specification of Bearing, the loads acting on the bearing may be radial, axial or angular. Ball and roller bearing may seem to have simple mechanisms but their actual operations are relatively complex. The materials used for bearings are designed to correspond to the intended use and will be discussed in the following section.

1.3 Bearing Materials

The complex design of bearings enables the movement with minimal friction also demands on advanced engineering within material selections where multiple demands are to be fulfilled, e.g. compressive strength, Fatigue strength, wear resistance and compatibility [1]. In order to meet the requirements, metals which are soft in nature have been used within bearings since their soft nature provides for a kind of “self-lubrication” or solid lubrication [1],[7]. With bearings commonly being built up in layers as discussed in previous section, each layer is consisting of different materials where the first is commonly made from either Babbitt, aluminum-based metal or copper-alloys [1],[6].

1.3.1 Copper-alloys

In comparison with babbitt, copper-alloys provide a superior fatigue strength with its higher hardness while other properties such as impact strength, bending properties, compactibility with other filler material shows inferior properties. Copper used for bearings are usually alloyed with tin as a strengthener and either lead or bismuth to provide a softer compatible phase [1], [7]. According to Yongyong, et al. [1] copper-alloys used for bearing materials can generally be divided into three groups. The first one contains lead in more amount, total about 30%, the second group contains lead in less quantity and also some amount of tin, 24% and 1,5% respectively. The third group contains much less lead, in total about 8% and somewhat more tin, 5% in total. However nowadays lead free options also exist. Compared to babbitt, the copper-alloy microstructure consist of a copper matrix with dispersed bismuth, tin or lead where copper dendrites are growing perpendicular to the surface [1],[9]. This kind of microstructure enables the bearing to have better capability to resist fatigue cracking, hence improving its superior fatigue resistance ability.

1.3.2 Aluminum-alloys

The aluminum-alloy bearings have the same usage as copper bearings having better corrosion resistant with good fatigue strength [1] . The aluminum alloy bearing be divided into three different groups containing various amounts of alloying elements; The first with a high tin and low copper content, 20% and 1% respectively. The second is low on tin and copper, with its 6% tin and 1% copper and the third group have high silicon and low copper content of 11% silicon and 1% copper. The alloys containing a lesser amount of silicon and tin is harder than other alloys and therefore requires a softer overlay than softer alloy. Additionally, when an insufficient corrosion resistant alloy is used an overlay then further improvement required to improve the corrosion resistant capability of the material. [1]

1.4 Inter layer and Overlay

For bearing materials where more protection is needed , top layers are deposited as per the requirement called interlayer and overlay. The no of layer can vary with variation in material also to acquire the desired characteristic. Both interlayer and overlay are deposited

mainly for improving friction resistance or corrosion resistant capability, depending on the bearing material requirement and working condition of the bearing. The coatings which are mainly used in overlay are lead, tin, polymer or sputtered materials. Lead overlay provides a surface which is softer and have low friction coefficient. It consists of minimum 10 wt% tin, providing the layer more corrosion resistant and better strength. Tin based overlays used contain about 4-6 wt% copper, which improves the hardness of overlay.

1.5 Lubrication

One of the most challenging task of the engineer is combination of material and lubricants to suits the desired need and effect the environment to minimum extend. Both materials and lubrications are selected to obtain the best final product and having its utility maximum. Research within the field of tribology and material research have provided the bearing industry with several types of lubrication alternatives to customize the specific need of the customer and its use in various fields For e.g., hydraulic oils, engine oils, turbine oils and gear oils respectively. Lubrication oil is not only the main thing to ponder about, the lubricant composition is a field of important criteria of selection due to various types of additives available in the market including; viscosity index improvers, detergents, , extreme pressure additives, foam inhibitors, antiwear additives and friction modifiers [9]. As detergents are mainly used to suspend particles and oxidize the products that cannot be miscible in oil and prevent oxidation and cladding [9]. For bearings where friction can be severe, wear reducers and friction modifiers are used to minimize the friction and decrease the wear effects. When the lubricant film thickness is more, it provides a sufficient distance between the surfaces which are undergoing relative motion, and thus helps in reducing the friction. When either load is increased or the speed decreased the full film thickness is reduced due to a dynamical film and frictional heat formed. Antiwear additives interact with the surface creating a solid protective layer which fills up the asperities while friction modifiers consists of long-chain molecules which physically absorbs on to the surface and provide the easily sheared lubricant film. Friction being one of the most important problems within e.g. bearings, lubrications a good lubrication helps in reducing the friction effects as mentioned. If a lubricant film having

sufficient thickness is present, friction can be significantly reduced and in some cases almost non-existent [10]. Within the field of lubrication these film-build-up's are commonly explained as various lubrication regimes, having different friction mechanisms and responsible for causing alterations in the coefficient of friction. These are commonly known as boundary, mixed and full-film lubrication regimes where the evolution of coefficient of friction can be described by a curve known as Stribeck curve.

1.5.1 Boundary lubrication

When the load is high or speed is low, the lubricant film thickness is small which causes the two surfaces to be in contact [8]. The lubrication regime is then called boundary lubrication, which is governed by asperity contacts entirely carrying the load and causing a friction increase [10],[11]. This regime provides the highest coefficient of friction of all three lubrication regimes which will be shown later in upcoming section. The antiwear and friction modifiers discussed earlier are here used to reduce friction and the risk of wear where formation of a small tribo chemical layer prevents asperities from welding together, hence minimizing friction and wear [14]. The film thickness parameter, λ , is a parameter which decide the thickness of lubricating film and in what regime a system is operating. In the boundary lubrication regime the film thickness parameter is the smallest, below 1 [10].

1.5.2 Mixed Lubrication

With decreasing load or increasing speed the system moves out of the boundary lubrication regime gets extended to mixed lubrication. The mixed lubrication regime is the transition between the boundary and full film lubrication regimes and the mechanisms carrying the load are a combination of the two, both asperities and lubricant film [10]. The film thickness parameter, is then in between the value of boundary and full film, namely $1 < \lambda < 3$.

1.5.3 Full-film lubrication

In cases when the lubricant film is sufficiently thick itself, solely carrying the load and separating the two surfaces the lubrication regime is called full-film lubrication. Within

this regime the coefficient of friction is low and occasionally it can be almost non-existent [12]. In the full-film lubrication regime the film thickness parameter is the highest, larger than 3 indicating a thick film formation. The full-film formed is directly dependent on lubricant viscosity and speed since a low viscosity and decreased speed prohibits a thick film formation [12]. The full-film lubrication regime can be divided into two separate groups, hydrodynamic- and elasto-hydrodynamic lubrication where the difference between the two is the influence of elastic deformation.

➤ *Hydrodynamic lubrication*

When the full-film lubrication regime is attained, the influence of both elastic and inelastic deformation can be present. In hydrodynamic lubrication (HL), the elastic deformation is sufficiently small to be considered as negligible and therefore the deformation occurring is solely inelastic. This type of lubrication is often encountered in journal bearings or thrust bearings where the lubricant pressure can be large enough to separate the two surfaces [7]. For hydrodynamic lubrication the lubricant viscosity, sliding speed and film thickness are important parameters influencing the lubrication and its efficiency [7].

➤ *Elasto hydrodynamic lubrication*

This type of lubrication is commonly occurring in non-conformal surfaces, a.k.a. counter formal, where the contact area is smaller. The small area results in large amount of pressure, amounting 1000 times more than the oil-film pressure of hydrodynamic lubrication [7]. With such amount of pressure, elastic deformation within the regime cannot be neglected, hence the name elasto hydrodynamic lubrication (EHL). In elasto hydrodynamic grease two sorts of regime exists; hard EHL and delicate EHL. Generally the material of the two surfaces decides the contrast between the two, in hard EHL, the materials included have high versatile modulii while materials with low flexible modulii fall in the classification of delicate EHL [7],[12].

1.6 Stribeck-curve

In the early 1900 Richard Stribeck presented his research in the field of experimental hydrodynamics showing that the minimum in coefficient of friction is a function of speed at different contact pressures [6]. Even though he was not the first to publish this correlation his name is today used to describe the dependency between the coefficient of friction as a function of speed, contact pressure and viscosity, also known as the Stribeck-curve [6]. This is mainly due to his publication in one of Germany's most highly regarded journals, *Zeitschrift des Vereins Deutscher (VDI, Journal of German Mechanical Engineers)*. The Stribeck-curve displays the relationship between coefficient of friction versus load and speed, sometimes plotted as the Hersey number, $H = \eta v / p$ (namely speed multiplied by viscosity, divided by contact pressure) or Shipper number, $Z = \eta v / PR$

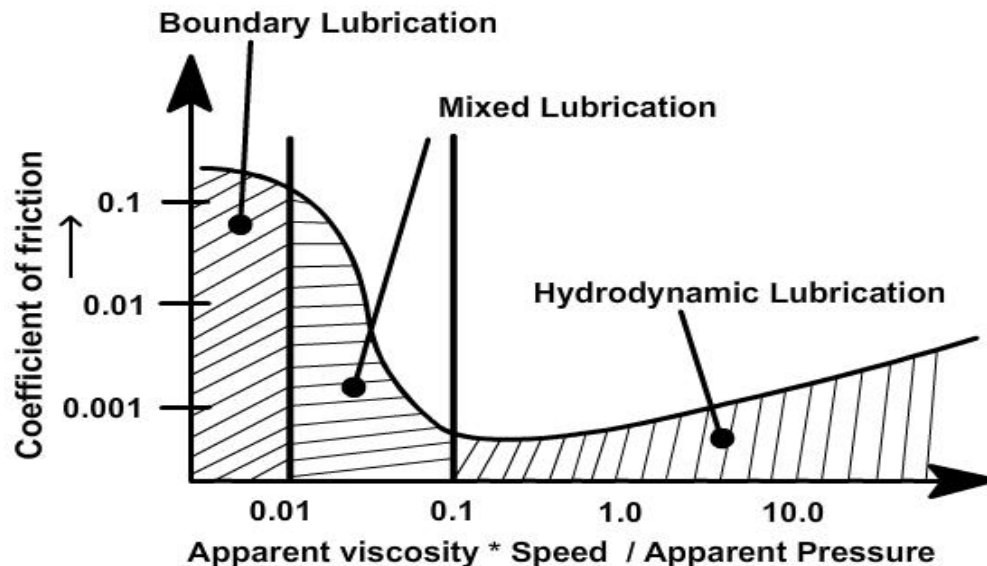


Figure 2: Stribeck curve [4]

a (where a raises the Average surface roughness of the hardest material) as can be seen in Figure 2. As the Stribeck-curve indicates the friction coefficient is high for low Hersey numbers. Within the first regime, the boundary lubrication regime, the film-thickness parameter is significantly low. On the opposite side of the curve, to the right, the coefficient of friction is low as the lubricant film is carrying the load. In between the

boundary and full film lubrication regimes, there is the requirement of mixed lubrication where the load is carried by both asperities and lubricant [12].

There are multiple parameters influencing the positions and shape of the Stribeck curve, where one important parameter is the surface roughness. When the surface roughness is more, the ratio of asperities and the surface is larger and the tips which are in contact with the counterpart surface have lower Hersey numbers compared to a smooth surface. Therefore either the velocity has to be increased or contact pressure has to be decreased in order to reduce the coefficient of friction and entering the mixed lubrication regime [9] This leads to a change in the Stribeck-curve and it is shifted to the right for surfaces with higher surface roughness providing that all other parameters remain the same as indicated by Figure 2.

1.7 Friction and wear of plain bearings

The wear mechanisms occurring in bearings are of various types, depending on the type of bearing and the mode of lubrication required as per the requirement. As mentioned in section 1.2, the various lubrication regimes for bearings and in particular plain bearings have different amounts of friction and wear. In boundary lubrications, the friction is higher since asperities in both surfaces are in contact while for full-film lubrication friction is greatly reduced [13]. In bearings experiencing full-film lubrication wear rarely occurs, besides from during start and stop due to insufficient lubricant flow or contaminating particles. Therefore a full-film lubricated bearing is more likely to fail from fatigue and not from wear [13]. The effects of alloying elements and surface aspects are important within wear of plain bearings and will be discussed in the following sections

1.7.1 Surface roughness's effects

Regarding wear and friction of plain bearings, the surface roughness has a great influence, regardless of the type of lubrication or the lubrication regime. Lundberg states [15] in his work that surface roughness has a higher dependency on lubrication than both viscosity and shear strength of the lubricant itself. In boundary lubrication, the surface

roughness is extremely important due to the load carrying mechanisms occurring. A rougher surface provides for an increase in friction. In full-film lubrication, the surface roughness effects on friction and wear is a function of the lubrication film thickness. A high viscosity lubricant can provide a thicker lubricant film and therefore a rougher surface is compatible with the film thickness and the effect is contrary for low viscosity lubricants.

1.8 Role of composites in today's era

In the past five decades considerable attention has been devoted to composite materials. A number of expressions have been suggested by which macroscopic properties can be predicted when the properties, geometry, and volume concentrations of the constituent components are known. The mechanical behavior of materials describes the response of materials to mechanical loads or deformation. The response can be understood in terms of the basic effects of mechanical loads on defects or atomic motion. The composites materials defined as the material who composed of two or more distinct phases (matrix phase and Reinforcing phase) and having bulk properties significantly different from those of any of the Constituents. Composites classified according to matrix and fillers or reinforcements. According to matrix it's classified as Metal matrix composites (MMCs), Organic matrix composites (OMCs) and Ceramic matrix composites (CMCs) and according to reinforcement classified as continuously and discontinuously reinforced composites. With the advancement of composites day by day, its uses increased widely in many areas like automobiles, aircraft, bio-medical, armor vehicles and many more. Metal matrix composites (MMCs) now-a-days have received increasing attention in the recent decades as engineering materials for industrial applications. The introduction of reinforcement into a metal matrix / metal alloy produces a composite material with an attractive combination of physical and mechanical properties and that cannot be obtained with monolithic alloys . Hence, MMCs are one of the main candidate materials for industrial applications in the aerospace, automotive and power utility industries. However, their mechanical and tribological properties such as strength, toughness, and corrosion and wear properties depend to a great extent on a number of factors of which matrix properties are very important.

1.8.1 Characteristics of Particulate filled MMCs

- *Inexpensive*
- *Conventional metallurgical processing techniques can be used for fabrication*
- *Enhanced strength*
- *Increased thermal stability*
- *Better wear resistance*

1.8.2 Advantages of Composites

- *Higher Specific Strength (strength-to-weight ratio)*
- *Flexibility of Design*
- *Resistance against Corrosion*
- *Investment is low*
- *High Durability*

1.9 Thesis Outline

The remainder of the thesis is described into following chapter:

Chapter-2: This chapter summaries various literatures available over a decade on mechanical and fracture characteristics of metal alloy, metal matrix composites .

Chapter-3: This chapter summaries the materials and methods of composite fabrication techniques, physical, mechanical and wear behavior of particulate filled metal matrix com

Chapter-4: This chapter summaries the physical, mechanical, fracture toughness of graphite and flyash particulate filled C93700 alloy composites

Chapter-5: This chapter summaries the study of surface morphology and sliding wear behavior of graphite and flyash particulate filled C93700 alloy composites

Chapter 6: Provides specific conclusions and summary drawn from experimental efforts of C93700 alloy composite and recommendations for future research in the field of composite Development.

Chapter 2: LITERATURE REVIEW

The purpose of literature review is to provide background information on the issues to be considered in this thesis and to emphasize the relevance of the present study. This chapter summaries various issues available over a decade on physical, mechanical, thermo-mechanical, fracture behavior and wear behavior of metal and metal alloy composites. The topics briefly reviewed still needs further research in order to improve the above said properties for industrial and structural applications. Also, several important parameters have been overlooked by previous researchers, among which are the types of reinforcements, geometry and size of the reinforcement etc. The following points are discussed keeping in view of our research works as Particulate filled metal matrix composites

- Study of ball bearing failure under various loading condition
- Effect of flyash and graphite filler content on mechanical properties and metal matrix composites.
- Effect of flyash and graphite filler content on fracture behavior of metal matrix composites.
- Effect of filler content on sliding wear behavior of C93700 alloy metal matrix composites.
- Summary of the literature survey and the research gap
- The objectives/aims for the research work

2.1 Study of ball bearing failure under various loading condition

Rolling element bearings are mostly used in machine to permit relative motion and support the load acting on the shaft . RCF fatigue is mainly developed due to the cyclic stresses at the contact surface of the bearing during performing the operation. Rolling contact fatigue includes high stress component under hydrostatic loading, tri-axial stress state and non-proportional loading and during cyclic loading changing planes of maximum shear stress, causes the sub-surface cracks. [16] Sliding forces are capable

of causing failure and results in the start of failure that propagate parallel over the surface and it may significantly reduce the bearing life. Rolling contact fatigue may divide into two categories, i.e. Surface initiated and sub-surface initiated.[5]

2.1.1 Wear and Failure of Bearing Surface

Roller bearing wear is caused by several reasons but the wear caused by fretting is mainly responsible for wear. Fretting wear can be classified in two types, i.e. corrosion due to contact surface and brinelling. Corrosion occurs between the bore of the bearing and the shaft. Fretting occurs inside the area of contact due to cyclic stresses. False brinelling looks like brinelling but it gradually disappears. Brinelling results in harmful effects caused over the bearing surface and indicating the indentations due to plastic deformation which is caused because of overload, it is mainly caused by the effects of severe vibration with improper mounting. Lubricant comes out from the contact area of raceways and rolling elements and it causes the direct metal-to-metal contact that results in wear. During the normal operation of the machine false brinelling does not occur, generally the vibration caused during the functioning of machine bearing results in fretting wear [17]. The rough surfaces produced due to false brinelling may result in excessive noise and may result in premature failure and also result in stress of the rolling element. In Figure 2 several defects are shown resulting over the shaft and cage of the bearing. The false brinelling can be identified as a dull surface with little trace of marks over the original surface finish with indentations, although the shaft can be subjected to brinelling effect by a very high load.[18]

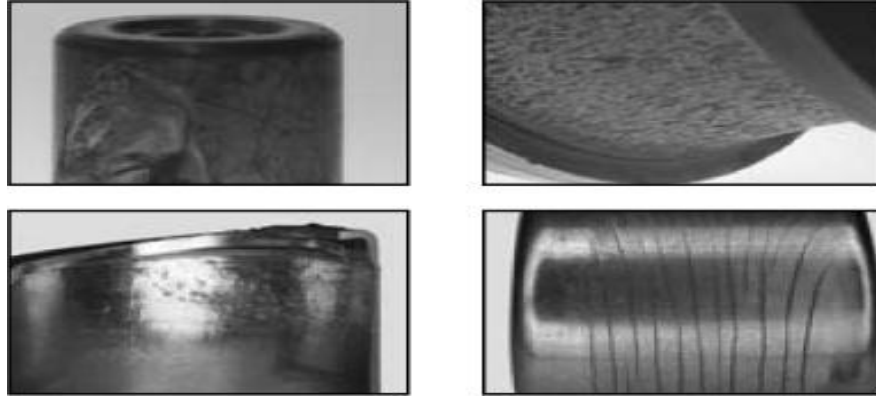


Figure 3: Brinelling and fretting wear of bearing

A.taqir et al after studying the cause of failure in aero engine and found that fatigue failure of the cage is one of the main cause for the failure of main bearing. He founded that it is clear that cyclic stresses were operative on the surface of cage along the band , where the deposited layer of dust or the ovality in the cage reduces the clearance and the cage was pushed against the outer race [19].

S.M. Muzakkir et al after investigating ball bearing used in sugar mills founded that the Journal Bearing using different lubricating oils have shown that applying lubricating oil with EP additives decreases the coefficient of friction significantly and also results in less amount of wear (weight loss). It has been observed that there is less amount of wear with clearance in the range of 0.1–0.20% of bearing radius.[20]

K.Gurumoorthy et al. after studying the handling practices of persons working with Bearing founded that it is important to note that the initial mounting practices must be implemented by the manufacturer of the equipment, such care may be absent during frequent reinstallation or servicing to acquire the rated life of the bearing. Examples of abusive handling that can negatively affect bearing life are as follows: tumbling the bearing onto a rigid surface, removing or installing the bearing with a hammering action instead of a press, pressing the bearing through the “non press fit” ring face, introducing contaminants during the process of handling or applying greasing operations, or damaging the cage or seal through impact. While some of these events

can occur at the early stage of bearing installation, they are far more likely to occur in servicing work centre of automobiles, due to insufficient training or poor tools.[21]

2.2 Particulate filled metal matrix composites

Metal Matrix Composites (MMCs) is one of the research area which is getting maximum attention in recent times for probable applications in aerospace and automotive industries and also in other industrial operation because of their better-quality strength-to-weight ratio and resistance at elevated temperature. The worldwide acceptance of particulate filled metal matrix composites (PRMMCs) for various engineering applications has been slowed down by the high cost of components required in production. This is the main reason for PRMMCs for getting the attracting and attention of automotive and consumer and commercial goods industries [22]. However, particulate MMC are used for numerous number of industrial application and these are mainly focused over Al and Cu alloy matrices while Titanium, Iron and Magnesium are based systems are also one of the major area of interest. The most commonly used particulates are Silicon carbide or Al_2O_3 but others (graphite, flyash, tungsten powder, garnet etc) are also used and have been investigated for alike purposes. The reason behind by lesser using the particulates are during the experimental process chemical reaction sometimes results in unfavorable results. For example Use of particulate silicon carbide results improper reaction in Cu and Ti-based MMCs and even during solidification silicon carbide can react with Ti matrix. Particulate MMCs are generally manufactured either by melting techniques and casting technique or by using powder metallurgy process. The other routes are including the processing by reaction or spray deposition technique can also be used. Quality control mainly focus on elementing the reaction taking place at interfacial surfaces, particularly through melting routes, and also the avoiding the defects in the micro structure such as weak interfacial bonding between crystal, voids in the composition and clustering of the filler at particular location. For using in structural application the size of the reinforcement particles are about 15-30 μm in diameter and constitute about 12 to 20 wt % .[23]

2.3 Effect of filler content on mechanical properties of metal matrix composites

Metal matrix composites (MMCs) have been acquiring increasing attention in the recent era as one of the major part for development of engineering materials. The use of reinforcement into a metal matrix can yield a composite material having a great combination of physical, chemical and mechanical properties that cannot be obtained with single alloys. Hence, MMCs are one of the primary candidate materials for development of various industrial applications which can be used in the aerospace, automotive and power generating industries. However the properties of composite such as toughness, strength, corrosion and wear properties depend to a great extent on a number of factors among which matrix properties are very important for proper development of new material[24]. The major purpose for producing metal matrix composites (MMCs) is to achieve light materials with high specific strength and stiffness. However, the main contribution to the increase in mechanical properties of PRMMCs is particle addition; it affects most of the properties of PRMMCs so far. The parameters related to the particles are volume fraction, size, shape and distribution of particles and among the selected parameters the most important parameter being the volume fraction. Park [25] was found that the composites have higher elastic modulus than the unreinforced alloy. The elastic modulus increased as particle volume fraction was increased but in a progressively decreasing rate. The composites have better tensile and yield strengths than the unreinforced alloy and also lowered ductility than the unreinforced alloy. The ductility decreased linearly with increasing particle volume fraction. Similarly, Poza [26] studied the microstructure of an 8090 Al-Li alloy reinforced with 15 vol. % SiC particles and after experimentation it was found that for the reinforced alloy processed with the same route founded that Sic particle prevents the grain elongation and thus provide a good surface with better grain homogenization and good isotropy of the system and these are mainly effected by property of material and reinforcement. The particulate reinforcements such as SiC, Al₂O₃ and aluminide are generally recommended to acquire higher hardness. The coating of reinforcements with Ni and Cu also results in development of good quality interface between particle and characterised in improving hardness. TiC when reinforced in Al matrix, results in improving hardness and weight ratio. Louis et al. [27]

after investigation founded that the improve in the hardness of the composites, containing hard ceramic particles not only depends on the size of reinforcement but also on the structure of the developed composite and nature of interface bonding.

K Rajkumar et al.[28] reported that hardness of hybrid composite decreases with increase in graphite content and wear rate of hybrid composite is decreased with increase in wt% of graphite and Tic .It was also observed that there is marginal increase in wear rate at high speed

R prieto et al.[29]observed that mixing the SIC with graphite is greatly influenced by the orientation of particle w.r.t to graphite plane. it was observed that conductivity of the particle is lower in the perpendicular direction namely 40w/mk while conductivity of the particle is higher in parallel direction w.r.t graphite plane say upto 500W/mk

Gongjun Cui et al.[30] discovered the synergistic effect of alumina and graphite on bronze matrix composite in sea water condition and he founded that alumina has strengthening effect on bronze matrix and he also observed that nickel coated graphite improve the interfacial bonding b/w bronze matrix and graphite.it was absorved that sea water shows lubricationg property but the wear rate is higher

Table 1: Overview of metal matrix composites mechanical properties

S.no	Matrix	Reinforcment	Methodogy	Mechanical properties	Reference
1.	A359	Al ₂ O ₃	Electromagnetic stircasting method	Al ₂ O ₃ increase by 2% up to 8% and this results hardness and tensile strength is increased and porosity is eliminated also results in refine grain structure. More Al ₂ O ₃ require more temperature for alloying	[33]
2.	AA6061	Titanium carbide	Stir casting method	Defect free aluminum matrix increase in specific strength. increase in wear loss is more with normal load but wear rate increased marginally	[34]
3.	Magnesium	SiC	Rheocasting process	Low porosity fraction with large particle high hardness value due to hard sic particle. There is	[35]

	AZD9 1)			Increase in yielding with decrease in ultimate tensile strength. Decrease in % elongation with decrease in hardness	
4	A356	Al2O3	Stir and compo-casting processes	The stress-strain curves show fracture strain decreases with increase in tensile strength and yield strength. The ultimate, yield and compression strength of the composite increase with increasing Al ₂ O ₃ content because of improvement in load bearing capability. Ductility increases with decrease in particle size. Compo casting results in more ductility	[36]
5.	Al-Cu alloy	Fly ash	Scanning electron microscope And stir casting	Base metal shows better fluidity than the composite. There is a decrease in overall density .There is increase in tensile strength as well as impact strength of the composite with increase in the flyash content and it is also founded that wear rate decreases with increase in the flyash content.	[37]
6.	5210 Al	(50%) of SiC particles	Powder metallurgy	There is increase in bending strength with increase in the amount of SiC particles.Proper grain orientation results in better tensile strength and also improvement in hardness	[38]
7.	Chilled cast al alloy	Quartz particulate	Cu blocks for chilled composite production	Chilled casting increase in wear properties, ductile fracture. sudden failure can be avoided, uniform particulate distribution	[39]
8	Al alloy	Delta alumina with silica binder	Vacuum filtration process	The ultimate tensile strength, elastic modulus and Rockwell hardness of the MMCs increases with increase in fiber length.	[40]
9	Al212 4-T1	SiC particles	Die casting	Fatigue strength of the material increases with increase in the capability to sustain the cyclic stress	[41]
10.	ZA-27 alloy	Short glass fiber	Liquid infiltration technique and destructive testing	The ultimate strength and Toughness of the material increases with fibre content while there is decrease in the ductility of the composite with increase in fibre.	[42]
11	Al-based	b-Al ₃ Mg ₂	Powder metallurgy	BA ₃ Mg ₂ reinforcement improves the mechanical properties of pure Al. There is increase in strength and compressive strength of the material in comparison to the base material.	[43]

12	Plain carbon steel	MoS ₂ \ MnS	Plasma transferred arc	Mos2 was found not capable in reducing the friction coefficient of the composite while Mns is capable of reducing the friction coefficient and thus improving the wear resistant at high loas and speed	[44]
13.	Al-based metal matrix	Zr-based glassy particles	Powder metallurgy	There is increase in compressive strength with increase in the amount of glassy particle but further increment results in decrease in the fracture strain of the composite	[45]
14	Al based	Zircon sand and silicon carbide	Two step stir casting process	Composite having Dual reinforcement each of the reinforced particles have different advantage in the composite. Silicon carbide improves the eutectic silicon and with the help of zircon sand interfacial bonding improves. Wear resistant of the dual reinforced composite also increases with the addition of dual reinforcement	[46]
15	Al15% Mg ₂ Si	Ni	Hot extrusion	Through tensile test it is concluded that tensile strength of the composite increases with increase in the Ni particle and also there is Improvement in corrosion properties.	[47]
16	Biodegradable Mg-based	MgO ceramics and Mg-Zn intermetallic	Electrochemical Measurements, immersion tests	Mg powder with ZnO powder at 550 C undergo reaction and start melting below the melting point of Mg, toand forms Mgo with the reduction Of Zno to zinc. Improves the melting rate and also results in good interfacial bonding with magnesium	[48]
17	Al-Mg	Amorphous silica particulate	High-energy ball milling process	Crystallization of the composite improves with the amorphous silica particle and no new formation of phases take place.	[49]
18	Al-based	Nanocrystalline Al-Ca intermetallics	Powder metallurgy	Sintering and compaction are formed with manual blending and it is observed that there is increase in impact strength of the composite and nano particle also results in better mixing with the base material	[50]
19	Al-based	Al ₄ Sr	Powder metallurgy and study of surface morphology	Improvement in microstructural property with improvement in mechanical property. Less generation of micro crack brittle nature was found to be converted in ductile characteristic.	[51]
20	Al-based	Al-Cu-Fe quasicrystalline particles.	Powder metallurgy	With the help of quasi crystalline particle there is improvement in mechanical property and compressive strength improve with addition of reinforcement.	[52]
21	Metal	Nano	Powder	Stress intensity factor was studied with the help of a	[53]

	matrix(al based)	particle*(Al ₂ O ₃ /Ni)	metallurgy	theoretical model and it is founded that nano particle results in improvement in dislocation mechanism.	
22	Iron based	TiC particle with Ni	Dual coating process	After testing it was found that nickel particle are homogeneously distributed inside the matrix .Tic particle induces better hardnesss and good abrasion resistance with improvement inn corrosion property with the help of nickel	[54]

H sarmadi et all.[31] founded the friction and wear performance of copper graphite surface composite fabricated by friction stir processing .it was observed that stir casting leads to more homogeneous distripution of particle and the triangular pin is most effective in distribution of particle.graphite contect lead to decrease in friction coffecient upto a certain values and graphite content also decreases adhesive wear.

K.palanikumar et all.[32] had performed the experimental investigation on analysis of thrust force in hybrid matrix of (al 15% SIC-4% graphite) composites and the most influencing factor of thrust force is the feed rate .

2.4 Effect of filler content on sliding wear behavior of metal matrix composites

Wear is a process of gradual removal of a material from surfaces of solids subject to contact and sliding.It mainly occur due to damage of the contact surfaces .Wear results in loss of material. Wear is unwanted and it results in decrease in reliability of industrial components. Systematic efforts in wear research were started in the 1960's in industrial countries.Wear Study is also a costly phenomena .The direct impact of wear results ibn replacement of worn parts ,decreases the Productivity rate and also causes indirect losses in the form of energy wastage and dumping of worn parts increases the enviromental burden[61].In the recent years researchers have taken great interest in study of the tribological process and are trying to reduce the wear as much as possible. For the development of high performance vehicle many properties should be there in material like lighter, stronger, stiffer, and more temperature and wear resistant[62].Wear can be defined as the gradual removal of material from solid surfaces as a result of mechanical action[63].To control the tribological properties (friction and wear) for aluminum

composites, done by controlling different factors which can be classified into two categories: one is mechanical and physical factors, and the other is the material factor[64]. The different tribological properties are widely used in the different applications as compared to mechanical properties. Many authors have investigated the friction and wear properties for copper composites that influences the following factors as [65]:

- The composite matrix and counter part of material with their hardness.
- The type of reinforcement with its shape, size and volume percentage.
- Different testing conditions (load, speed, temperature, lubrication, environment conditions, etc.)

Asthana [66] studied about the processing effect on different physical and mechanical properties of cast metal matrix composites by using kind of solidification and casting techniques. He found that to establish a rigorous protocol between both fabrication technique and properties of composites, we have to evaluate the composite performance in synergy with fabrication techniques

Tribological behavior of self lubricating Al_2O_3 20Ag₂0CaF₂ composites have been investigated by Jin et al. [67].They investigate in their report that during sliding condition plastic deformation plays an important role in the formation of lubricating film on the sliding surface. Similar, investigation about the wear behavior of SiC reinforced with Si₃N₄- and Al₂O₃-matrix composites was report by Dogan and Hawk [68]. They found that by the addition of SiCp in the aluminum matrix improved the tribological environment of the composites. Lead base alloy are used in many applications due to its excessive properties like low initial cost, excellent foundary castability and fluidity, good mechanical properties as compared to other alloys.

Dinesh A. et al. [69] investigate the dry sliding wear behavior for hybrid metal matrix and have performed the optimization by using taguchi technique.Different parameter are studied to reduce the uncontrolled factor influencing the sliding wear characteristic and to enhance the dry sliding wear of metal matrix composite. In their study they found that the wear rate, load and sliding speed of the composites are highly influenced by wear factor i.e. sliding distance.

Mahendra and Radhakrishna [70] studied about the fabrication and wear behavior of Al–4.5% Cu alloy reinforced with fly ash content which is produced by using conventional foundry technique. Different wt.-% (5, 10 and 15 wt.-%) of fly ash content were used to added in molten metal. From the investigation they found that the resistance to dry wear and slurry erosive wear increased with the increasing in content of fly ash in composites also the corrosion resistance increases with increasing in fly ash content

2.6 Research Gaps

The gaps which are observed from the literatures are:

Only few scholars have taken C93700 and it's composite for the purpose of exploring it for industrial application. Also, the dual reinforcement (Flyash and graphite) with C93700 alloy is rarely reported.

Properties and fracture toughness behavior is also rarely reported, especially in relation to particulate filled metal alloy composites. Only few researchers study on thermal mechanical behavior of graphite and flyash filled metal alloy composite .Only fewer literatures are available on study regarding fracture behavior of metal alloy and their particulate filled composites.

2.7 Objective of the present work

- Based on the available literature survey presented in this thesis and obtained various research papers advantages and disadvantage the following objectives are proposed in the present thesis. Fabrication of flyash and graphite filled C93700 alloy composites by vaccum casting techniques at five different weight percentages of Flyash and graphite filled composites. Study of physical and mechanical characterization of unfilled and particulate filled C93700 alloy composite by experimental means.
- Evaluation of surface morphology of the particulate filled metal matrix composite.
- Sliding wear behavior of Fly ash and graphite particulate filled alloy composites have been studied under control multiple varying condition of speed and load.

- Evaluate the effect of surface roughness on wear and friction of particulate filled metal matrix composite and determination of variation in coefficient of friction(μ) with variation in sliding speed and load.
- Optimization Of wear performance by using method of Taguchi

Chapter summary

This chapter provides literatures which are available over a decade on different mechanical and fracture characteristics of metal matrix composites . The research gap which are given above providing the objective for this current work. The next chapter discusses different methodology of composites material

Chapter 3: METHODS AND METHODOLOGY

In this chapter describes the different methods and materials which are used to complete the thesis work. Different fabrication methodology, properties of selected materials and material characterizations (tensile, impact, hardness, XRD, SEM, fracture toughness, Steady state wear behavior analysis), are explain in this chapter by experimental procedure.

3.1 Properties of selected materials

3.1.1 Matrix Material

For the development of composite C93700 (lead tin bronze) is used as matrix material. C93700 has got great machining properties, good corrosion resistance and capable of withstanding mild acids attacks as found in sea water. Bearings manufactured with C93700 have good wear resistance under high speed environment, heavy load and vibration due to cyclic loading and also have low friction which help in operation during boundary lubrication..

Table 2: Physical property of C93700 Alloy

Different properties	Metric
MELTING POINT – IN LIQUID STATE	929 C
MELTING POINT – SOLIDUS	762 C
INCIPIENTION OF MELTING	316 C
DENSITY	8.86 GM/CM ³
SPECIFIC GRAVITY	8.86
ELECTRICAL RESISTIVITY	16.95
ELECTRICAL CONDUCTIVITY	0.059 MEGASIEMENS/CM @ 20 C
THERMAL CONDUCTIVITY	46.9 W/M · °K AT 20 C

COEFFICIENT OF THERMAL EXPANSION	18.5 · 10 ⁻⁶ PER °C (20-200 C)
SPECIFIC HEAT CAPACITY	377.1 J/KG · °K AT 293 K
MODULAS OF ELASTICITY IN TENSION	75800 MPA
MAGNETIC PERMEABILITY	1.0

Table 3: Mechanical property of C93700 Alloy

Properties	Value
Hardness(Brinell Hardness)	60
Tensile Strength	35(KSI)
Yield Strength	20
Elongation(% in 2 inch)	20

The various types of grades available are C937,C932,C935,C938,C943.All the grades are classified as high leaded tin bronze having varying amount of alloying element which are copper,lead and tin.

3.1.2 Reinforcing Materials

➤ *Flyash*

Fly ash is one of the residues which is generated in combustion of coal and consist of the several heterogeneous material such as SiO₂, Al₂O₃, Fe₂O₃ are the main chemical components which are present in the fly ash. Flyash can be used in many ways such as alumina reinforced spheres. Fly ash can also be mixed with molten metal and cast to reduce the density and weight of the composite, and this is mainly because of low density of fly ash. Fly ash particles are cheap as they are generated as industrial waste. In this study, fly ash particles used are generated through combustion of coal is chosen as reinforcement material. In India coal produces about 1100 lacks tons of fly ash per year from burning about 2500 lacks tons coal for power generation [2]. Present days fly ash utilization improved and reduces the pollution in environment, now in present day's fly ash is

focusing and improving their investigating in various fields like MMCs, bricks, agricultural and etc. By adding fly ash reinforcement with commercially copper to make copper fly ash composite is improving their properties in strength and hardness and reduces the weight of the commercially copper. Hence, composites with fly ash reinforcement are overcome the cost barrier for wide applications. By adding of commercially copper with fly ash is decreases the need of intensive energy-copper, by resulting in energy savings [3]. By mixing the copper fly ash composites by using stir casting process method, in stir casting process is mixing conventionally in directly furnace it will reduce the time for mixing the copper and fly ash. Mixing the copper with fly ash particles in the ratio of 5% to 20% of weight in the commercially copper. To studied on commercially copper and fly ash chemical analysis in testing Laborites. Hence, studied before and after physical and mechanical properties of copper fly ash metal matrix composite and also comparing with pure commercially copper. The copper fly ash composite are mainly used in aerospace, industries and other engineering application.

Table 4: Chemical analysis of flyash

Different Composition of flyash	Weight Percentage
Silicon dioxide (SiO ₂)	68
Aluminum oxide (Al ₂ O ₃)	29
Iron oxide (Fe ₂ O ₃)	0.10
Calcium oxide (Cao)	1.6
Magnesium oxide (Mgo)	1.3



Figure 4: Images of Flyash Powder

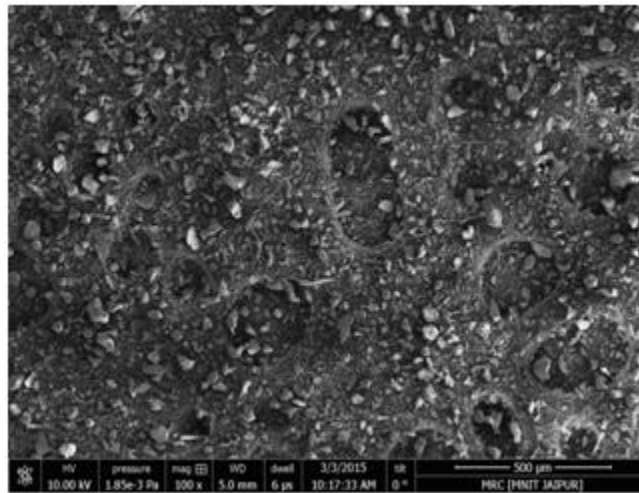


Figure 5: SEM of Flyash Powder

➤ *Graphite*

Graphite is made up of carbon atoms just like diamond and both are allotropes of carbon. Graphite is one of the most stable form of carbon occurring in natural condition.. Graphite may be found the highest grade of coal such as anthracite and also meta-anthracite,. Graphite has a layered, planar structure. In each layer, the carbon atoms are arranged in lattice structure having honeycomb shape and are separated with .145 nm, and the distance between the plane is 0.336 nm. Atoms in the plane are covalently bonded with some of the

bonding sites potentially satisfied with other atoms. The fourth electron is free to move in the plane, making graphite good electrical conductor. Bonding between layers is weak due to vander wall bond and this mainly results in capability of graphite layer to slide over one another and thus have better lubricating action.

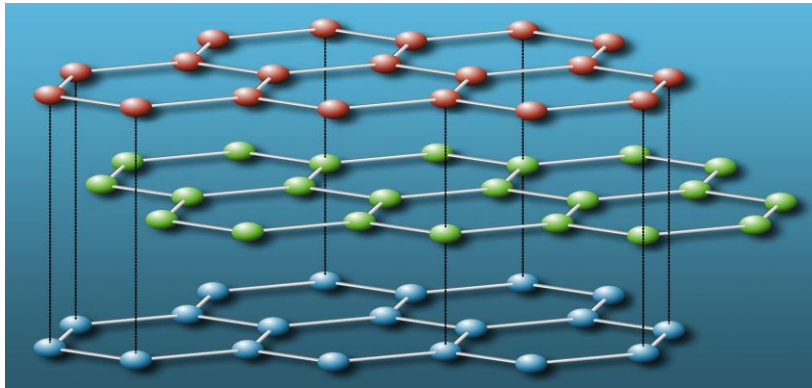


Figure 6: Arrangement of graphite in layer form

There is a common belief that graphite's lubricating properties are mainly due to the loose inter lamellar coupling between the layer structure. But it has been found that lubricating action of graphite is reduced in vacuum environment. Thus environment plays an important role in functioning of graphite.[4]



Figure 7: Images of graphite (i) powder form

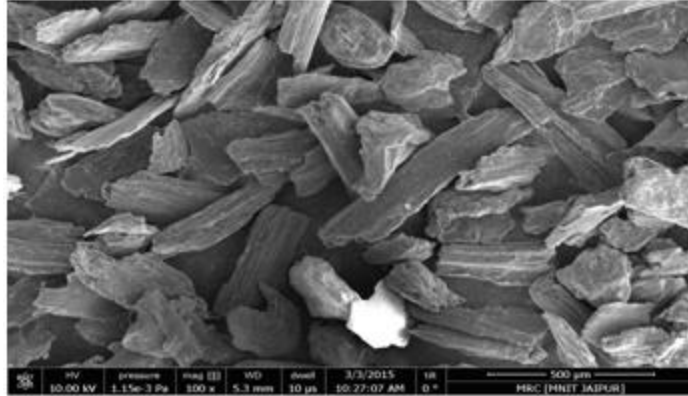


Figure 8: SEM of Graphite powder

Self lubrication of the graphite is due to fluid action of air and moisture over the graphite surface it has been found that graphite can perform very well in the moist environment and can retain its lubrication at high temperature .

Table 5: Physical Property Of Graphite

PROPERTIES	GRAPHITE
Apparent density	1.80
Hardness	40
Compressive strength	55
Flexural Density	28
Modulus of elasticity	10
Thermal Conductivity	85
Temp limit in air	455

3.2 Fabrication Method

Casting Of Composite is Performed On Vacuum Chamber Die Casting.

The Set up can Be Explained As Below:

The C93700 alloy based metal matrix composites were designed as per given table (Table), amounting to 100% by weights and prepared using Vaccum chamber die casting technique.

Vaccum Casting is a liquid state fabrication technique; in which dispersed phase (reinforced particles)and C93700 Alloy Chips Are used as Matrix Material and for the reinforcement



Figure 9: Images of vaccum chamber die casting

Flyash and Powdered Graphite were used and varied as per the sample preparation is mixed with C93700 alloy (melting temperature of 1250°C achieved using vaccum furnace setup and graphite crucibles are used for pouring the metal matrix and filler into the mould,the proper mixing of reinforcement with metal matrix is obtained by manual stirring for 2-3 minute. The mixture is then poured into a permanent mold and allows cooling to room temperature.

Table 6: Design of fabricated particulate filled C93700 composite

Samples Prepared	Wt% of C93700	Wt % Of flyash	Wt% of Graphite
1.	100	0	0
2.	96	2	2
3.	94	2	4
4.	92	2	6
5.	90	2	8

3.2.1 Preheating Of Reinforcement

Preheating Is Always Desired For Proper Mixing Of the Reinforcement And To prevent The Thermal Coagulation

For Preheating Equipment Used Is Shown Below:



Figure 10: Furnance for preheating the reinforcement

3.2.2 Sample Preparation For Performing The Experiment

➤ *Removal of Oxides and scales from the Plates*

For removing the scales from the Surface of the plate Surface Grinding operation has been performed. It uses an abrasive rotating wheel to remove the layer of oxide and scale formed over the surface.



Figure 11: Surface grinding operation



Figure 12: Plate after Surface Grinding

➤ *Cutting Of Samples*

Cutting of plates for the sample preparation is performed by using bend saw cutter which consist of a circular rotating blade for performing the cutting operation.

3.3 Physical and Mechanical characterizations

3.3.1 Void Content

The void content of the said composites are computed by using equation given below.

$$\text{Void Content} = \frac{\text{theoretical } (\rho) - \text{experimental } (\rho)}{\text{theoretical } (\rho)}$$

Where, ρ represent the density of composite. The rule of mixture equation is used for calculating theoretical density and for the actual density, it is calculated by Archimedean principle of weighing the sample first in air and then in water.

Voids are considered defects in composite structures and there are several types of voids that can form in composites depending on the fabrication route and matrix type.

3.3.2 Hardness

Hardness is the property of a material that enables it to resist plastic deformation, usually by penetration.

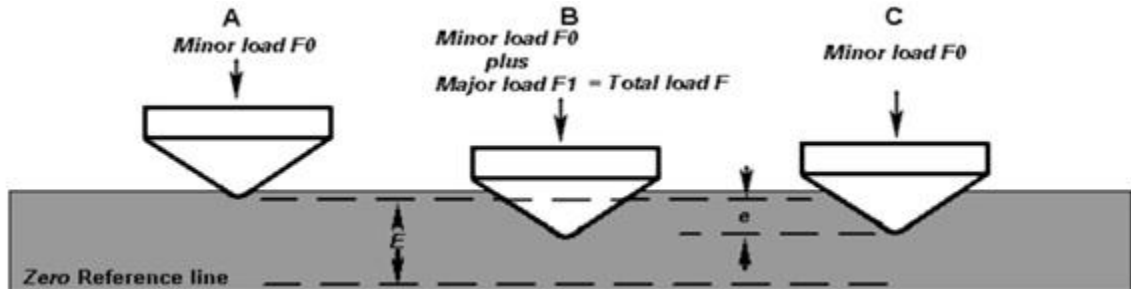


Figure 13: Rockwell Principle



Figure 14: Rockwell Equipment

However, the term hardness is defined as ability of material to resist bending, scratching, abrasion or cutting. Hardness the Rockwell hardness of the composite is determined. The

Rockwell hardness test method consists of indenter in the shape of diamond cone or steel ball to study the hardness of the material by the depth of indentation.

3.3.3 Tensile Test

To determine the different composition materials tensile test following ASTM D 3039-76 is carried out on a flat rectangular specimen with straight end tab of 150 mm × 10 mm × 10 mm and a span length of 75 mm, at 2mm/s cross-sectional speed. For the test, universal testing machine (UTM) Electronic Tensometer is used . The material properties C93700 (Young's Modulus = 64 GPa, poisson ratio = 0.34).



Figure 15: Electronic Tensometre

3.3.4 Flexural Test

The flexural strength of the given composites is determined using universal testing machine (UTM) . The standard size of specimen is 50 mm × 4 mm × 4 mm with span length of 40 mm at 2mm/s cross sectional speed. The flexural strength is given by Eq. 2. $FS = \frac{3WL}{2bt^2}$ Where, W is the maximum load, b is the width of specimen and t the thickness of specimen and L is the span length of the sample.



Figure 16: Universal Testing Machine

3.3.5 Impact strength

The impact strength test is done by Charpy and Izod Impact tester. The standard specimen for impact test is $55 \times 10 \times 10$ mm and the depth under the notch is 10.2 mm. The equipment consists of a hanging hammer pivoted with the help of a needle after placing the workpiece the hammer is released to strike the workpiece and the energy required for breaking the material is indicated by the rotation of the spindle.

Impact tests are used in studying the toughness of material. Toughness can be defined as the capability of material to absorb energy before undergoing failure. Brittle materials have low toughness as they can sustain very little amount of plastic deformation. The impact value of a material can vary with the change in the working environment. Lower temperature results in less impact strength of the material.

The size and nature of the specimen can also affect the value of the Charpy impact test due to different imperfections in the material and different grain orientations which result in stress raisers in the material and can change the value of the Modulus of toughness.



Figure 17: Charpy Impact Test Equipment

3.4 X-Ray diffraction Analysis (XRD)

X-Ray powder Diffraction analysis is a powerful tool in studying the crystal structure of various element present in the composite, the peak of the material indicate the highest percentage of the material present in the composite lesser peak indicates lesser percentage of material. By the maximum value of angle we can know about the structure of the element. The value of wavelength of X ray and the bragg relationship can give the value of different planes of miller indices and thus in this way by knowing the different planes we can know about the shape of the material. For example copper has got the fcc structure can be verified by the value of plane as (1,1,1) and for this the the BRAGG relationship is indicated by $L = 2 d \sin \alpha$ Where, L is the wavelength of the X-Rays, d is the distance between different plane of atoms in the crystal lattice, α is the angle of diffraction.



Figure 18: XRD equipment used to perform the experiment

According to Solís [76] the use of surfactants helps in obtaining materials with higher area, which are performed by homogeneous crystallite sizes. Brij [35] investigated nano metric crystallite sizes of 4.4 and 6.2 nm, respectively. Powder XRD analysis indicate the various crystalline phases present in the material. The effect of XRD is conducted over calcinated and non calcinated glass which exist in amorphous state the diffraction peaks are obtained between the angle range of 20 to 40.

3.5 SEM (Scanning electron microscopy)

Nova Nano FE-SEM 450 (FEI) is capable of generating ultra high resolution characterization & analysis of various material on a precise nanometer scale information. Advance optics study with electron beam can be performed with the help of lens TLD-SE & BSE, DBS & STEM. This lenses are capable of providing high resolution image. Beam landing energy can go down from 30kev to 50ev. It gives a resolution of 1.4 nm at 1 kv (TLD-SE) & 1 nm at 15 kv (TLD-SE). The EDX detector is attached to study the different chemical composition of the composite because each element has a particular binding energy which is indicated by the help of electron beam emitted from the material.



Figure 19: SEM equipment used to perform the experiment

3.6 Sliding Wear Test

The Pin-On-Disc Tester (Magnum) is used to test the friction and wear characteristics of dry or lubricated sliding contact of various types of materials including polymers, composites,

ceramics,metals, different lubricants, action of cutting fluids, coatings and heat-treated samples.

The test is performed with the help of rotating disc whose speed can be varied as per the requirement and it is rotated against the stationary specimen for a specified period of time. After the experiment the mass loss is calculated and during experiment temperature can also be varied and can be performed in ambient condition and also in inert condition with the help of nitrogen gas.

The normal load, rotational speed, and wear track diameter can be adjusted in accordance with ASTM G99 test standard . Wear disc diameter –160mm (En31 disc 55-60 HRC).Several types of holders are there to hold the various types of specimen such as Cylindrical or rectangular.



Figure 20: Figure Equipment used to perform sliding wear test (pin on discTribometre)

3.7 Process optimization and Taguchi method

Taguchi is a statical method which is generally used to reduce the uncontrolled factor and to eliminate the least significant parameter influencing the particular phenomenon. The goal in any experimentation process is to characterize the relationship between response and a set of factors that influence the response. This can be achieved by conducting experiments and analysing the data. Sliding Wear is one of the such process in which a number of controlled factors collectively determine the output performance of material i.e the Wear

rate. Hence, for the present work a statistical technique called Taguchi method is used to optimize the process parameter influencing the wear rate of C93700 alloy composite and to eliminate the least significant parameter.

For performing any experimental research the procedural cost is very high and it become a difficult situation to analyse all the controlled factor moreover it also become a lot more time consuming process. Taguchi method is one of the most important tool to statically determine the least influencing parameter with very less amount of test to be conducted. This method involves development of the experimental conditions using specially constructed tables known as ‘orthogonal arrays’. Use of orthogonal arrays significantly reduces the number of experimental configurations to be analysed . The conclusions drawn from small scale experiments can be implemented over the entire experimental drspace and can study the effect of all control factors over the area of optimization. The most important stage in the design of experiment lies in the selection of the control factors. Therefore, in this work, to explore the possible effect on wear rate the factors considered are reinforcement , load , sliding velocity and sliding distance. Thus, the impact of four parameters is studied using L₂₅ orthogonal design. These four parameters each at five levels would require 5⁴ = 625 runs in a full factorial experiment whereas Taguchi’s experimental method reduces it to 25 runs only offering a great advantage. The experimental observations are transformed into signal-to-noise (S/N) ratios. There are several S/N ratios available depending on the type of characteristics are available but here we are using smaller is better as we have to reduce the wear rate.

Smaller-the-better’ characteristic : $\frac{S}{N} = -10 \log \frac{1}{n} (\sum Y^2)$

Table 7: Orthogonal array for L25 experiment

Expt.No	A (Reinforcement)	B (Sliding Velocity)	C (Load)	D (Sliding Distance)
1	1	1	1	1
2	1	2	2	2
3	1	3	3	3

4	1	4	4	4
5	1	5	5	5
6	2	1	2	3
7	2	2	3	4
8	2	3	4	5
9	2	4	5	1
10	2	5	1	2
11	3	1	3	5
12	3	2	4	1
13	3	3	5	2
14	3	4	1	3
15	3	5	2	4
16	4	1	4	2
17	4	2	5	3
18	4	3	1	4
19	4	4	2	5
20	4	5	3	1
21	5	1	5	4
22	5	2	1	5
23	5	3	2	1
24	5	4	3	2
25	5	5	4	3

Chapter summary

This chapter briefly explains properties of selected ingredients for this research work, their compositional combination variables, fabrication methodology, various testing for physical and mechanical characterization (density, void-fraction, hardness, tensile, flexural, impact, fracture toughness and X-ray diffraction) by experimental means. The next chapter presents the mechanical characteristics C93700 alloy and its particulate filled composites under study.

Chapter 4: PHYSICAL AND MECHANICAL CHARACTERIZATION OF COMPOSITES

This chapter presents the physical, mechanical and fracture toughness of C93700 alloy composites by experimental method.

4.1 Effect of dual reinforced alloy composites on void content

The theoretical density and experimental density of dual reinforced alloy composites are calculated by using Archimedes principle and void content is then calculated. These equations are given below-

$$\text{Void Content} = \frac{\text{theoretical } (\rho) - \text{experimental } (\rho)}{\text{theoretical } (\rho)}$$

Table 8: Theoretical and Experimental density of Dual reinforced C93700 composites

S.no	Composition	Theoretical Density(gm/cc)	Experimental Density(gm/cc)	Void Content (%)
1.	0% flyash+graphite	8.860	8.591	3.03
2.	2% flyash+graphite	8.820	8.588	2.630
3.	2% flyash+4% graphite	8.780	8.576	2.315
4.	2% flyash+6% graphite	8.720	8.527	2.210
5.	2% flyash+8% graphite	8.650	8.486	1.890

4.1.1 Theoretical and Experimental density of Dual reinforced C93700 composites

In this work flyash and graphite reinforced C93700 composites system has been studied with particle size of 80-100 μm for all the the samples of composites of C93700 alloy

composites at five different (0 – 8 wt.-%) weight percentages. The magnitude of experimental density remains comparatively lower than the theoretical density as shown in Table 4.1. The reinforced composites show lower density than C93700 alloy and further it decreases with increasing in (Flyash and graphite) content. It is observed from Table1 that with the increase in filler content the void function of all the alloy composites decreases. This may be attributed to the fact that theoretical consideration is based on idealistic assumptions that differs experimental calculation. The void content should be as minimum as possible, it occurs due to proper interfacial bonding between the reinforcement and matrix.

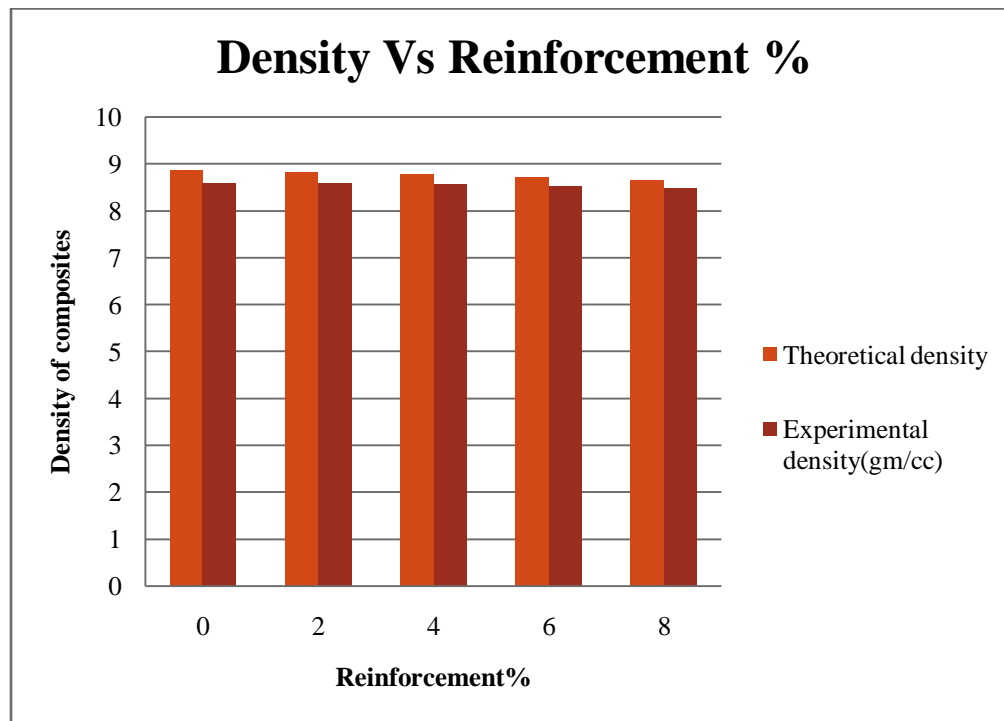


Figure 21: Experimental and Theoretical density of dual reinforced C93700 alloy composite

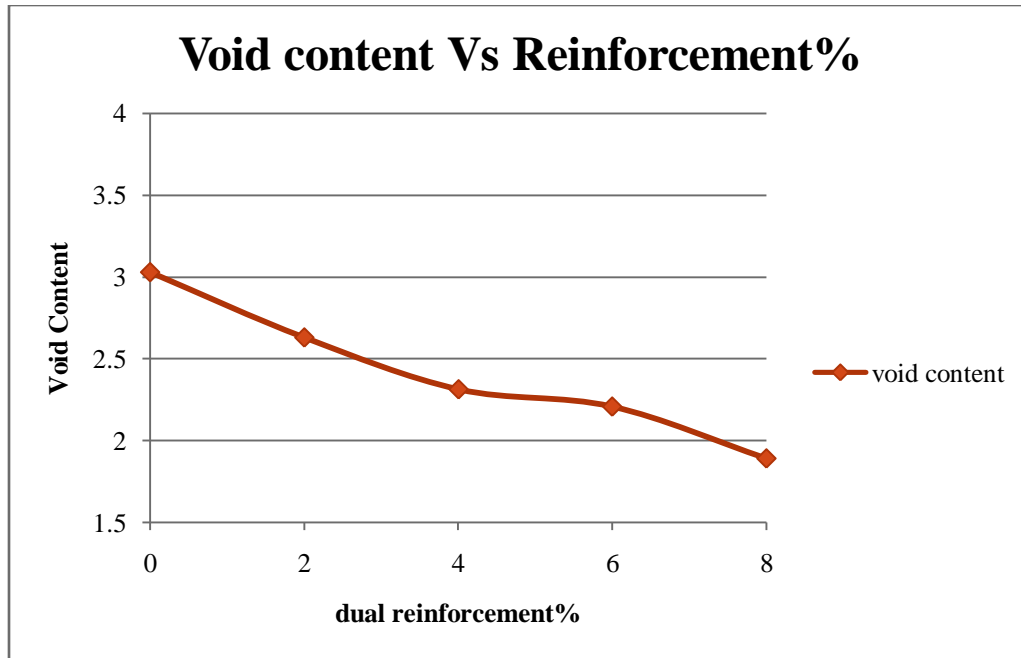


Figure 22 Effect of void content on C93700 Alloy composites

Figure 22 shows the graph between void content and wt.-% of fly ash and graphite filled C93700 alloy composites. It shows that the with increasing in the wt.-% of filler content the void content become reduces, it may be due to the homogeneous interface between reinforcement and matrix material.

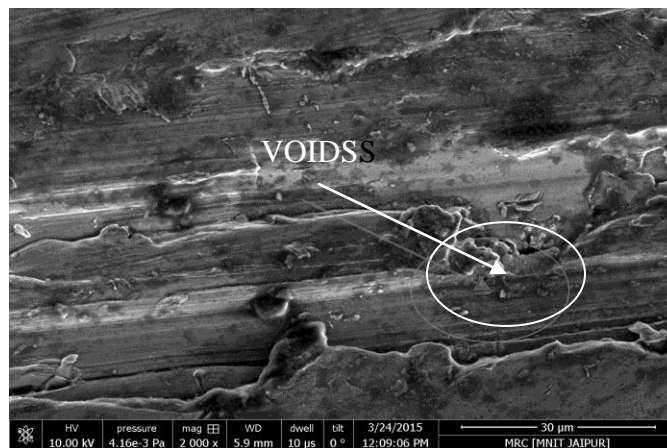


Figure 23: SEM Images of 0wt% dual reinforcement

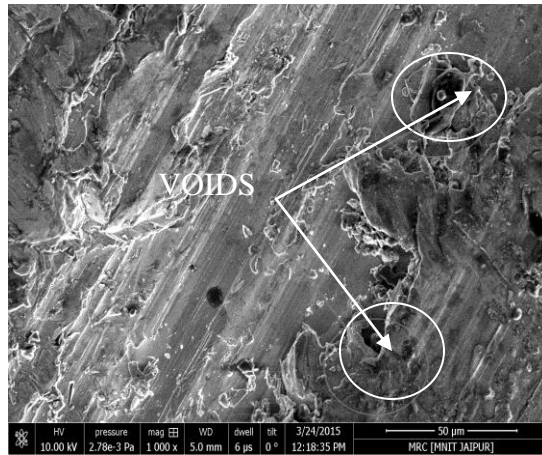


Figure 24: SEM images of 2wt% dual reinforcement

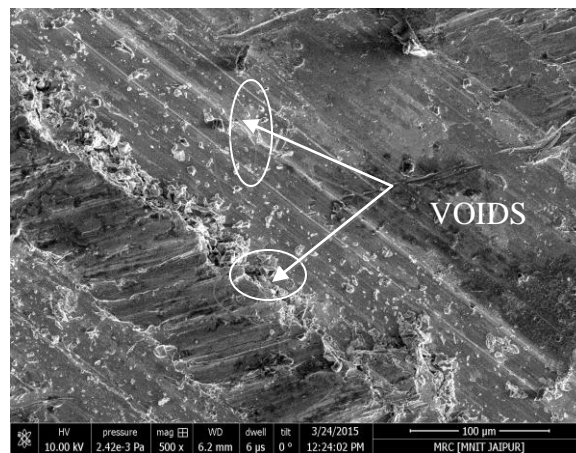


Figure 25 :SEM images of 4wt% dual reinforcement

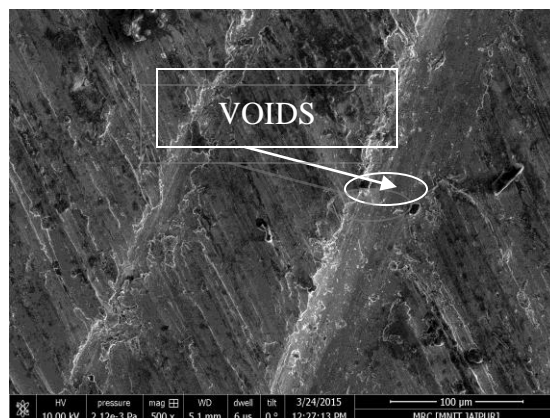


Figure 26: SEM images of 6wt% dual reinforcement

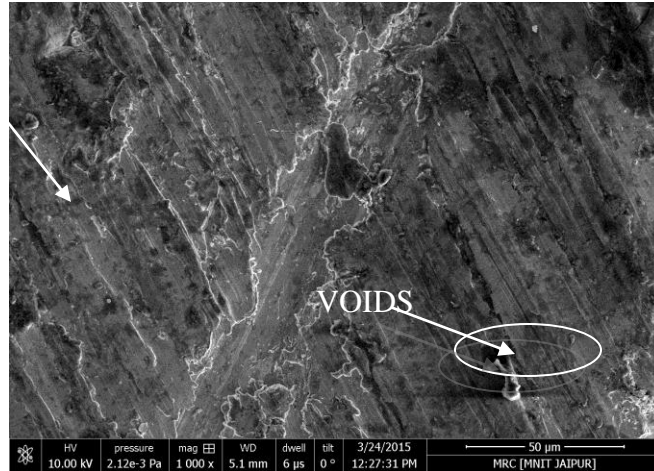


Figure 27: SEM images of 8wt% dual reinforcement

The volume percent of porosity was measured by comparing the theoretical and experimental densities determined by the Archimedeian method . Sajjadi [93] conducted experiment and founded that with increasing in micro and nano alumina the void content for micro filler increase and with the help with nano particle void content reduces. The nano particle also results in less agglomeration and shows better fusibility with the base material

4.2 Effect of C93700 dual reinforced composites on hardness

From Table 8, the value of hardness of dual reinforced alloy composites is evaluated experimentally. The hardness of the composites increases with the increment in wt.-% of filler upto 2% and then it gradually decreases on increasing the content of graphite keeping the wt.-% of flyash constant in each sample.

PURE	2%	4%	6%	8%
62	66	64	62	60
61	67	65	61	62
63	69	63	62	59

S.no	Composition	Hardness
1	0%flyash+graphite	62
2	2%(flyash+graphite)	67.33
3	2%flyash+4% graphite	64
4	2%flyash+6% graphite	61.66
5	2%flyash+8% graphite	60.33

Table 9 Hardness(Rockwell B of C93700 alloy matrix composite

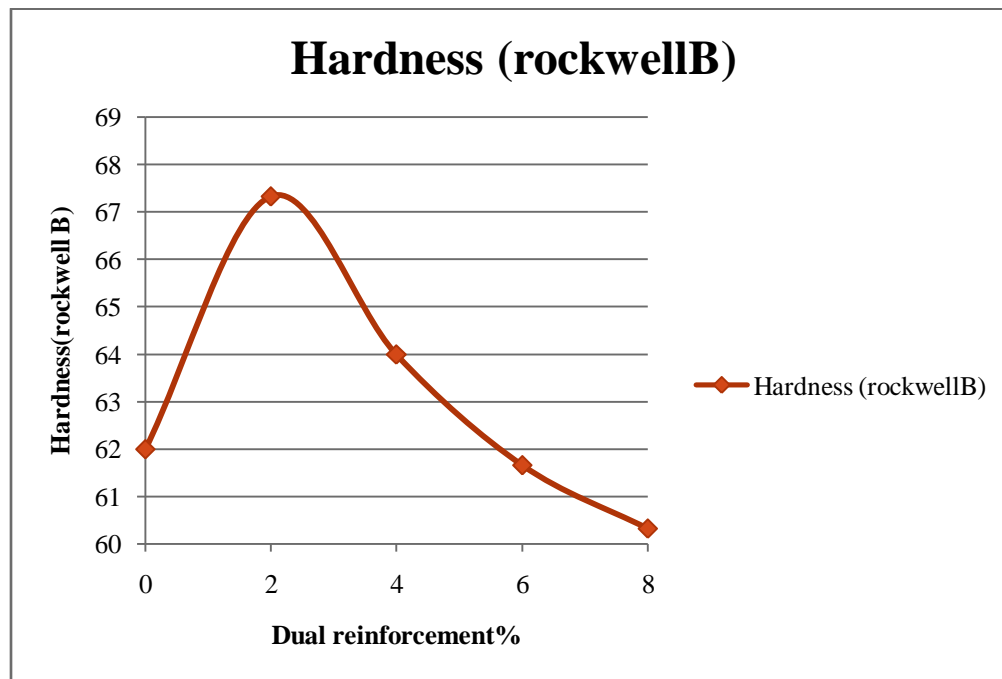


Figure 28: Effect of hardness graphite and flyash filled alloy Composites

4.3 Effect of C93700 dual reinforced composites on tensile strength

The tensile strength results for the different wt.-% dual reinforced C93700 alloy composites are shown in Figure . This study was evaluated by experimental method by performing the tensile test on UTM. The tensile test performed on the samples shows that increasing the amount of graphite filled in the metal matrix keeping the amount of flyash constant (wt%=2) increase the tensile strength of the material upto(wt%=6) but after that increasing the amount of graphite results in the decrement in the value of tensile strength.

V.V.Ganseh, N.Chawla[71] Founded that anisotropy of the material reinforcement also determine the Tensile strength of the material the orientation can be parallel or perpendicular to the applied load and he founded that reinforcement which is perpendicular to the plane orientation provide more strength to the material.

Table 10 : Tensile Strength Of C93700 alloy Composite

Dual Reinforcement%	Tensile Strength
0	240
2	255
4	283.5
6	296.5
8	287

A.ramesh et all compared the mechanical property AL6061/Albite and AL6061/ Graphite metal matrix composites and he founded that addition of graphite particle increases the tensile strength of the material upto defined limit and further increment lead to decrease in tensile strength.

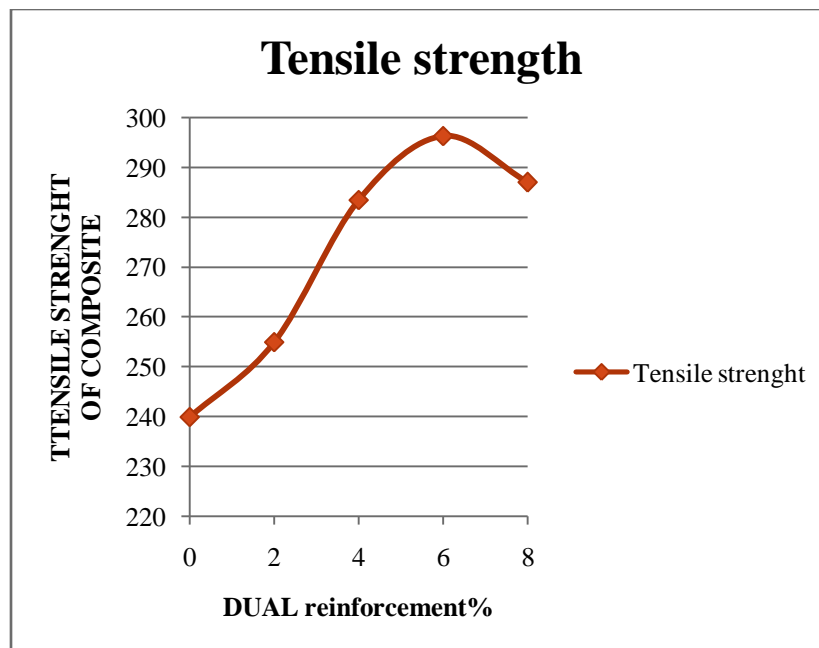


Figure 29 :Tensile Strength Of C93700 alloy Composite

4.4 Effect Of fly ash and graphite on the young's modulus of composite material

Yong's modulus is one of the very important property which determines the strength of the material subjected to various kind of loading. After performing the experiment on the UTM upto the elastic limit for different samples it has been founded that increasing the amount of graphite and flyash in the metal matrix of C93700 alloy leads to increase in the value of Young's Modulus but it has been found that the increment is gradual after(wt%=6).

T. Mochida et all[72] Performed the experiment on particulate filled metal matrix composite and it was observed that many mechanical property of PRC composite is dependent on the nucleation of the filler in the metal matrix.It was observed that homogenization of the filler inside metal matrix leads to better mechanical property such as Young's Modulus and fracture strength.

Table 11 : Youngs' Modulus Of C93700 alloy Composite

Dual Reinforcement%	Young's Modulus
0	117
2	141
4	176.25
6	223.5
8	242

Youngs modulus generally indicate the variation of the stress with the strain and it also shows the yielding capability of the material .It generally determine the material extension or compression limit during tensile load or compressive load it indicate the elastic capability of the material to prevent the plastic deformation with the applicataion of load.A material having higher Youngs Modulus is stronger than material having less Youngs Modulus.

Youngs modulus changes with the orientation of the material .For homogeneous material the property can be same in all direction .In composites due to different particle at different

position the value of Young's Modulus can vary along Different Direction. It also depends on the direction of force Application. For example carbon fibre are much more stronger when loaded in parallel direction but not capable of sustaining load when loaded in perpendicular direction.

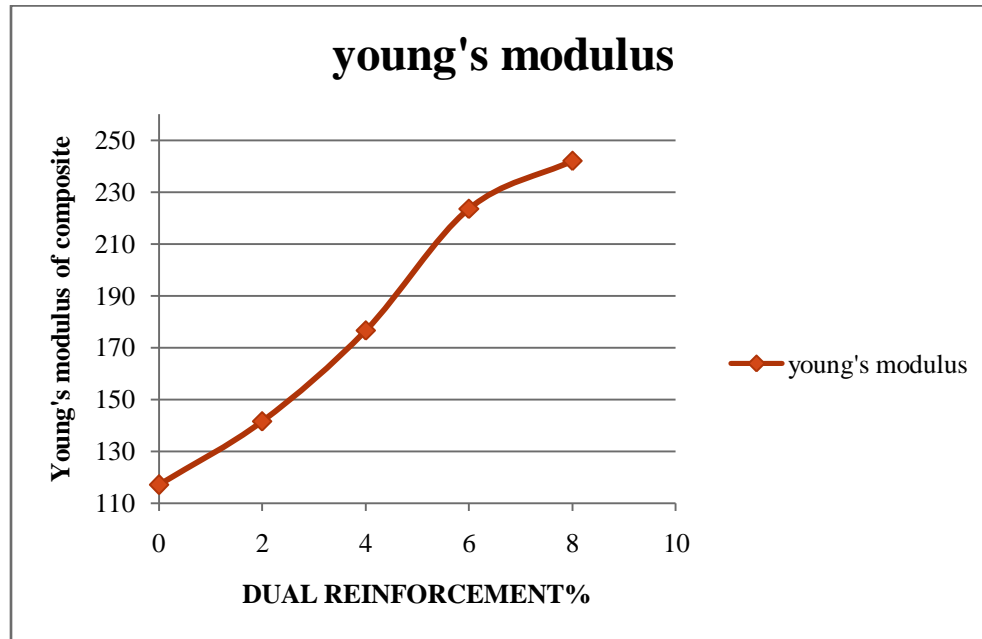


Figure 30 : Youngs' Modulus of C93700 alloy Composite

4.5 Effect Of fly ash and graphite on the Compressive strength of composite material

Compressive strength is one of the major requirements for all the material which are used in the condition where they are subjected to compressive load. Generally the brittle material are strong in compression but there are many places where the high compressive strength is required in ductile material, for ex-material used in ball bearing and gears. After performing the compressive test on the samples using universal testing machine it has been observed that addition of flyash and graphite in C93700 alloy composite leads to increase in the compressive strength of the material.

The compressive strength is the ability of the material to withstand the load applied in such a way which results in reduction in size of the material .It can be measured by plotting applied force against % of deformation in a Universal testing machine. Different material shows different compression limit some reaches the maximum limit other may fail early because of anisotropy of the Material.

Table 12: Compressive Strength Of C93700 alloy Composite

Dual Reinforcement%	Compressive Strength
0	90
2	95
4	97.8
6	99.5
8	98

When Tensile load is applied atoms of the material moves apart and whwn compressive load is applied the atoms moves closer to each other .In both the situation material try to comes to its original position and thus material opposes the cause resulting in the change of its equilibrium position.

The "strain" is the relative change in length under applied stress; positive strain results due to tensile loading and negative strain is caused due to compressive loading .More deflection in compression results in buckling.

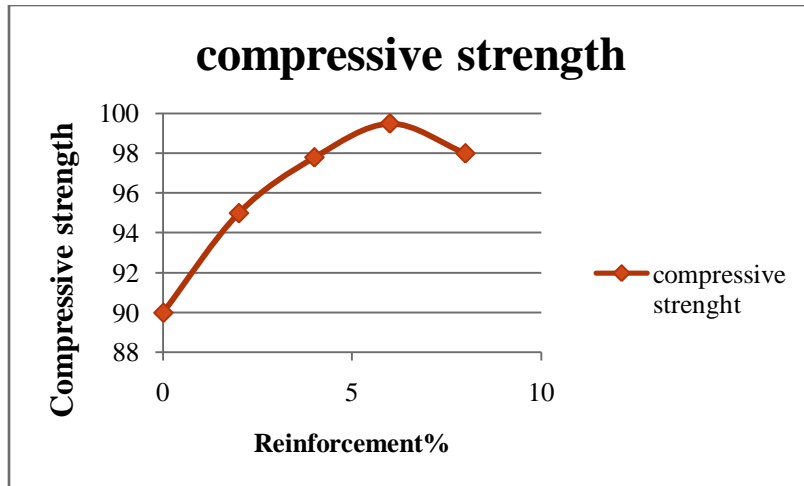


Figure 31 : Compressive Strength Of C93700 alloy Composite

4.6 Effect of fly ash and graphite on the Ductility of composite material

Figure 32 is a graph showing the reinforcement content on the ductility of C93700 graphite and fly ash particulate composites (measured in terms of percentage elongation). As the content of dual reinforcement the ductility of composite increases and further increment in the content of fly ash and graphite leads to further increase in the elongation %. This increase in ductility is due to graphite which acts as a good solid lubricant [73], and it facilitates the movement along the slip planes. Increment in ductility is due to the presence of soft graphite phase which reduces the embrittlement effect which occurs due to localized stress at the interface of matrix interface with the reinforcement.

Dual Reinforcement%	% elongation
0	2.0
2	3.18
4	5.27
6	6.23
8	6.94

Table 13 : Ductility of C93700 alloy Composite

Ductility of the metal is very high due to metallic bond which are present between the atom and does not obstruct the movement of the atom along the slip plane thus resulting in higher amount of ductility and this is one of the main reason for using metal matrix for development of composite requiring higher ductility.

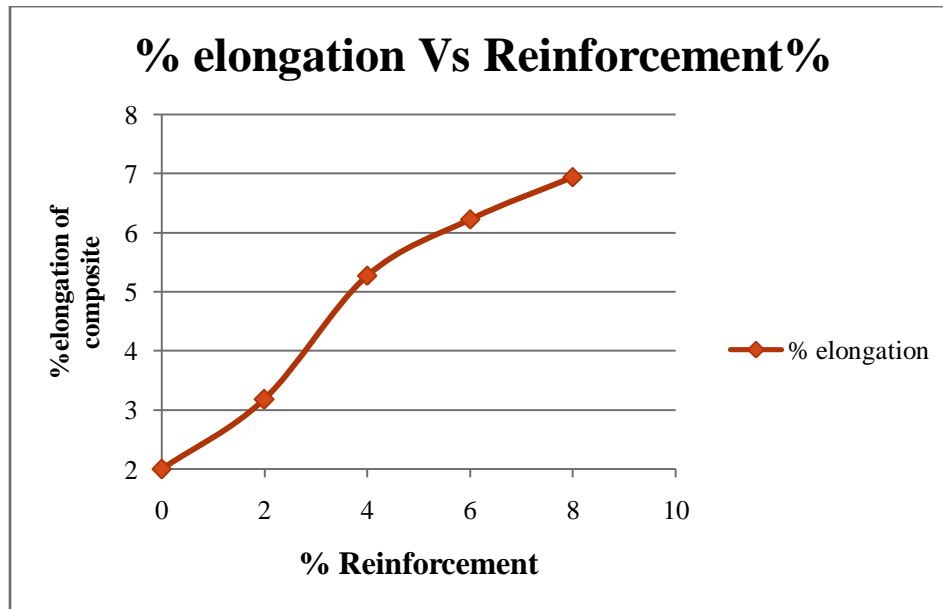


Figure 32: Ductility of C93700 alloy Composite

4.7 Effect of fly ash and graphite on the Flexural Strength of composite material

The flexural strength plot shows that, the flexural strength increases with the increase in fly ash and graphite particulate filled alloy composites. Figure shows the flexural strength for the different composition of composite i.e. dual reinforced alloy composites. It is found experimentally that for pure alloy the flexural strength is lower and it increases with increasing the composition of filler in composites. The flexural strength of the specimens increases with increase in addition of filler but it has been found that the flexure strength increase gradually up to 6% but further addition results in very small increase in the flexural strength of the composite. Melendez [74] studied that by increasing the manufacturing temperature, the flexural properties of all TiMMCs (Titanium matrix composites) decreased. In particular, titanium matrices reinforced with NDs exhibited better flexural properties

then composites reinforced with CNTs. It was very significant after HP at 900°C, being the high flexural strength for TiMMCs with NDs up to 1473 MPa compare to 947 MPa for TiMMCs with NDs. However, after HT the differences between the flexural strength of both types of TiMMCs are insignificant. The higher HT temperature used, the lower flexural strength measured in both types of TiMMCs. Susanna Segerström et al.[75] founded that flexural strength of the polymer composite increases upto 47% and after that increase in filler content results in the decrease in the flexural strength of the composite.

Table 14 : Flexural Strength Of C93700 alloy Composite

Dual Reinforcement%	Flexural Strength
0	260
2	275.3
4	287.50
6	293
8	294.50

RG slutter et al. after conducting experiment on flexural strength of steel and Concrete founded that the flexural strength for a homogeneous material is same as tensile strength but for composites due to heterogeneous nature it can vary along different direction of loading because the slip planes along different direction will oppose different amount of restraint to the deformation. The flexural load generally effect the extreme fibre with higher stress so that part will undergo failure firstly while tensile failure can take place from anywhere as the stress is equally distributed through the phase

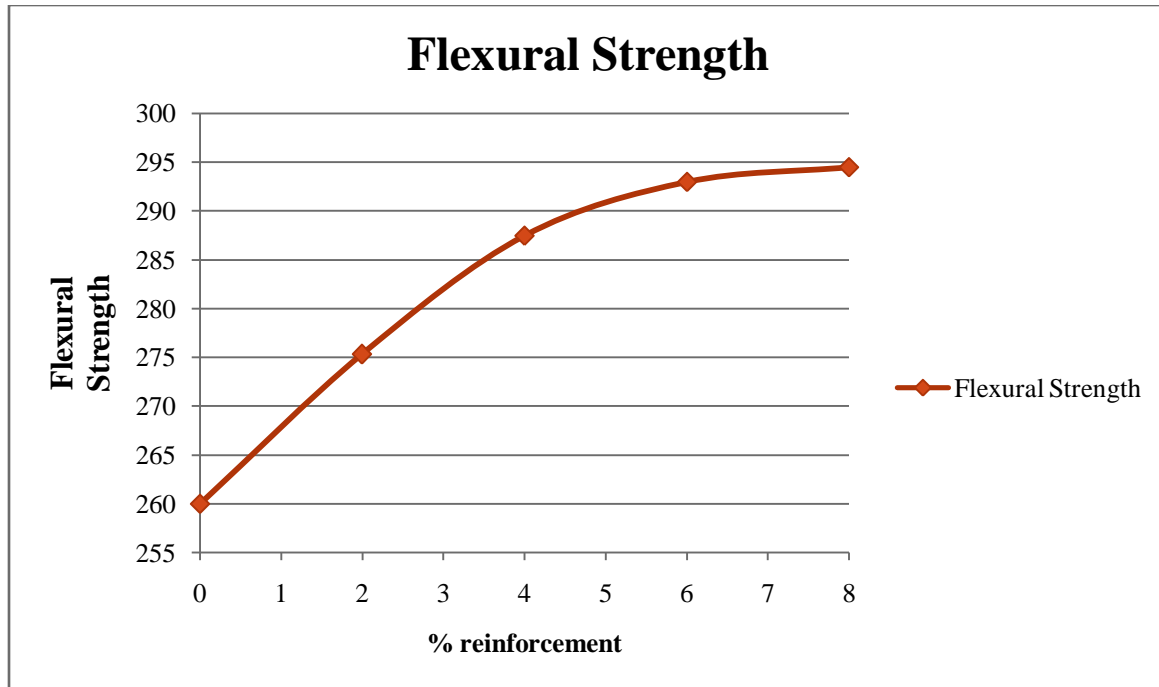


Figure 33: Flexural Strength Of C93700 alloy Composite

4.8 Effect Of fly ash and graphite on the Impact Strength of composite material

The impact strength (in terms of impact energy absorbed in Joules during the Izod impact test) of the given composites improves with addition graphite and flyash filler (Figure 4.19). The impact strength is increased with the increasing in reinforcement upto (4%)weight percentages, it also shows that the uniformly distribution occurred in between particulate filler and C93700 alloy composites. Further increase in the amount of the dual reinforcement results in the decrease in the value of the Impact strength. Impact strength is one of the property which greatly influences the toughness of the material which determine the maximum stress observing of the material before fracture.

Table 15 : Impact Strength Of C93700 alloy Composite

Dual Reinforcement%	Impact Strength
0	28
2	36
4	40

6	38
8	34

The notch preparation is one of the most important task to acquire the best result. The dimension of the notch must be prepared carefully as the plain strain caused in the material will determine the result.

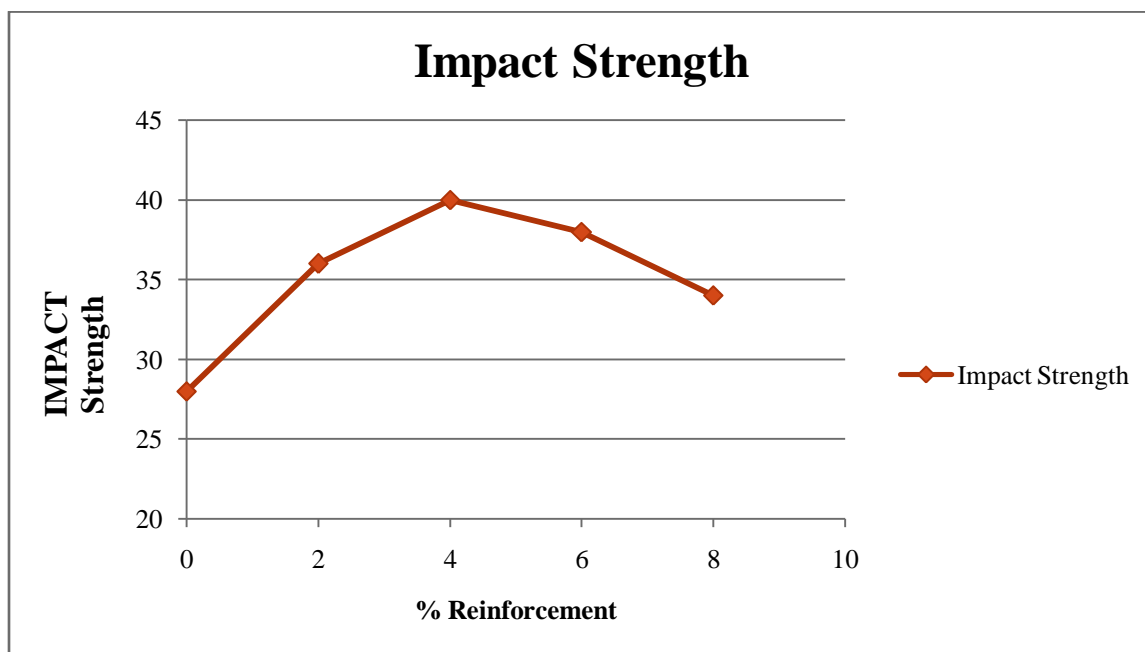


Figure 34 : Impact Strength Of C93700 alloy Composite

4.9 Effect of reinforcement on coefficient of friction under steady force with variation in sliding speed.

Coefficient of friction is one of the important factor which influences the material capability to perform on the sliding surface. With decreament in the coefficient smooth motion take place between the surface undergoing relative motion w.r.t each other but increase in the value of μ leads to rubbing between the material more and more and leads to loss of material

thus the value of μ is very important in determining the durability of any material. Here it is found that with increase in amount of the graphite and flyash in C93700 alloy matrix leads to decrease in the value of μ . Though it is found that with increase in the sliding velocity the coefficient of friction reduces but the decrease is maximum for the 4% (graphite and flyash) filler content.

Gongjun Cui et al. Also studied the Tribological properties of bronze-graphite composites under sea water condition and he founded The graphite is an effective solid lubricant in sea water environment. The composite containing approximately 11.7 wt% nickel coated graphite has the best tribological properties in sea water environment. The nickel coated graphite composite show lower friction coefficient in sea water.

Table 16 : coefficient of friction of C93700 alloy Composite under steady force with variation in sliding speed

velocity	A0	A2	A4	A6	A8
1.047	.34	.32	.28	.25	.23
2.094	.26	.24	.23	.22	.18
3.140	.24	.22	.21	.18	.21
4.186	.22	.20	.20	.20	.20

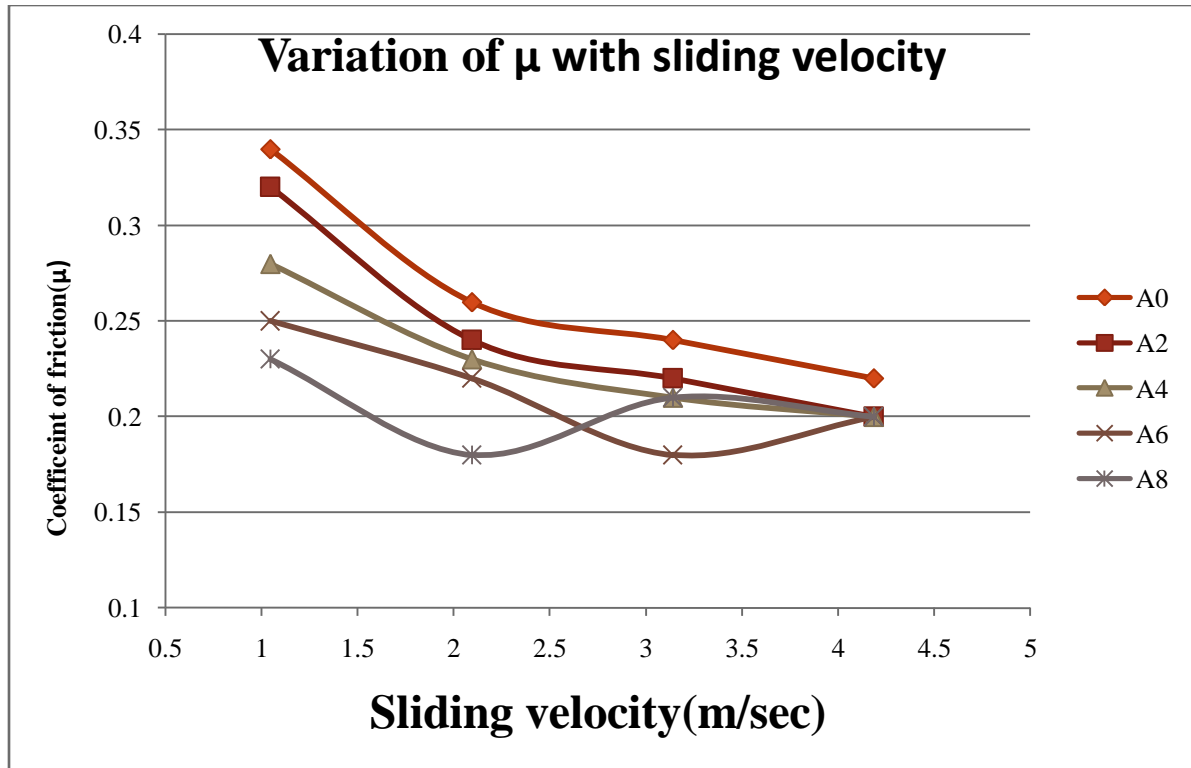


Figure 35: Coefficient of friction Of C93700 alloy Composite under steady force with variation in sliding speed

4.9.1 Effect of reinforcement on coefficient of friction under steady velocity with variation in Load

Load is also one of the important factor in determining the workability of the material under various varying condition. coefficient of friction is also greatly influenced by the variation of load. By performing the experiment on pin on disc tribometre under steady velocity of 1.047 m/sec(200 rpm) it has been observed that increase in the amount of reinforcement leads to decrease in the coefficient of friction but it has been found that there is gradual increase in the the coefficient of friction for 2% (A2)(graphite and filler content) and then after there is decrease in the value of μ with increase in the load. For 4%(A4) wt content of graphite and filler particulate it has been observed that there is increase in coefficient of friction when Load increase from 25 N to 35 N and then it gradually decreases eith increase in load.Further addition of dual reinforcement leads to decrease in the value of μ with increase in load. The decrease in coefficient of friction can be explained as graphite smear out of the matrix at higher applied loads.

Table 17 : coefficient of friction under steady velocity with variation in Load

Load	A0	A2	A4	A6	A8
5	.30	.25	.24	.22	.20
15	.28	.23	.23	.23	.18
25	.25	.24	.21	.21	.19
35	.24	.21	.22	.20	.18
45	.22	.20	.18	.17	.16

M. Kestursatya et all. Studied the Wear performance of copper/graphite composite and a leaded copper alloy and he founded that that increase in graphite content lead to decrease in coefficient of friction with increase in load.

After rubbing of material the deposited film break up and the clean surface come in contact. Due to contact between two surfaces heat generation take place at the point of contact and this also effect the frictional force between surface of two material But with the help of graphite and flyash which acts as a good heat absorber the effect of temperature can be minimized and it will prevent the increase in the value of coefficient of friction thus allowing less wear rate at higher speed.

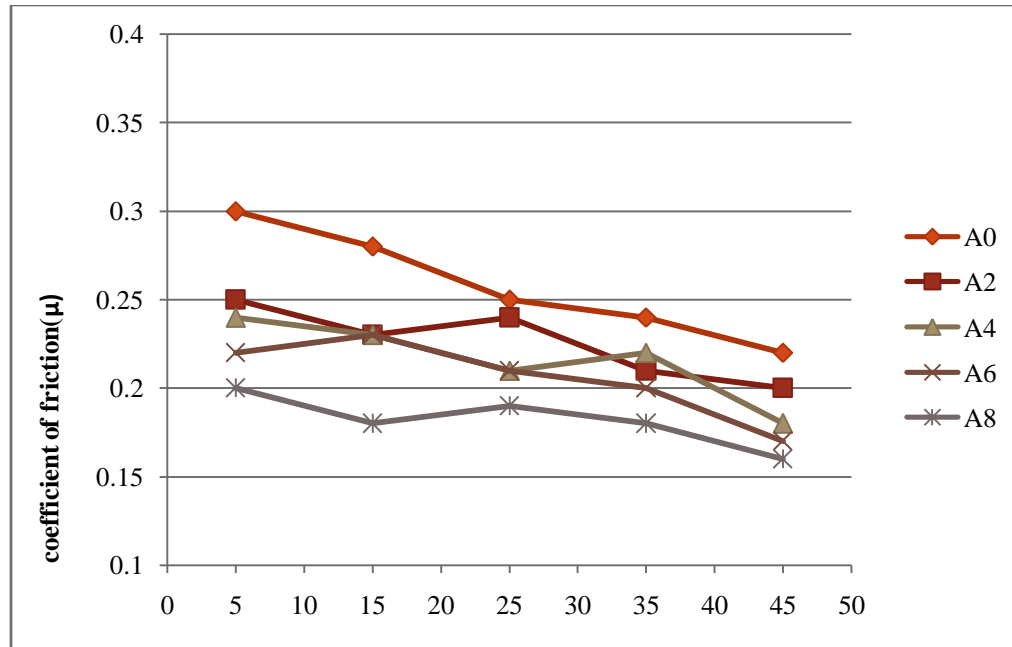


Figure 36: coefficient of friction under steady velocity with variation in Load

4.10 Effect of reinforcement on Wear loss(mass loss) under steady load with variation in sliding velocity

Wear loss which is indicated in loss in mass of the object undergoing any relative motion w.r.t another surfaces. Wear loss is one of the important criteria for determining the wear rate of any material over a period of time. On performing the wear test of the graphite and flyash filled C93700 alloy matrix under steady load of 15 N with variation in the sliding speed it has been observed that for A0 and A2 with increase in velocity the wear rate increase but for A2 the slope of wear rate is steeper in comparison to A0. For A4 the wear loss increase with increase in velocity but the wear loss is less at higher sliding speed and this is due to the ball bearing effect of the flyash and self lubricating action of the graphite which decreases the wear rate.

Gongjun Cui et al. founded that Tribological properties of bronze-graphite composites under sea water condition. The nickel coated graphite composite show lower friction coefficient and specific wear rate in comparison with the uncoated graphite composite containing the same graphite content but there is decrease in wear rate with addition of graphite.

Table 18 : Wear loss (mass loss) under steady load with variation in sliding velocity

velocity	A0	A2	A4	A6	A8
1.047	.009	.007	.004	.002	.002
2.094	.011	.010	.007	.005	.004
3.140	.014	.012	.008	.007	.007
4.186	.016	.013	.010	.009	.008

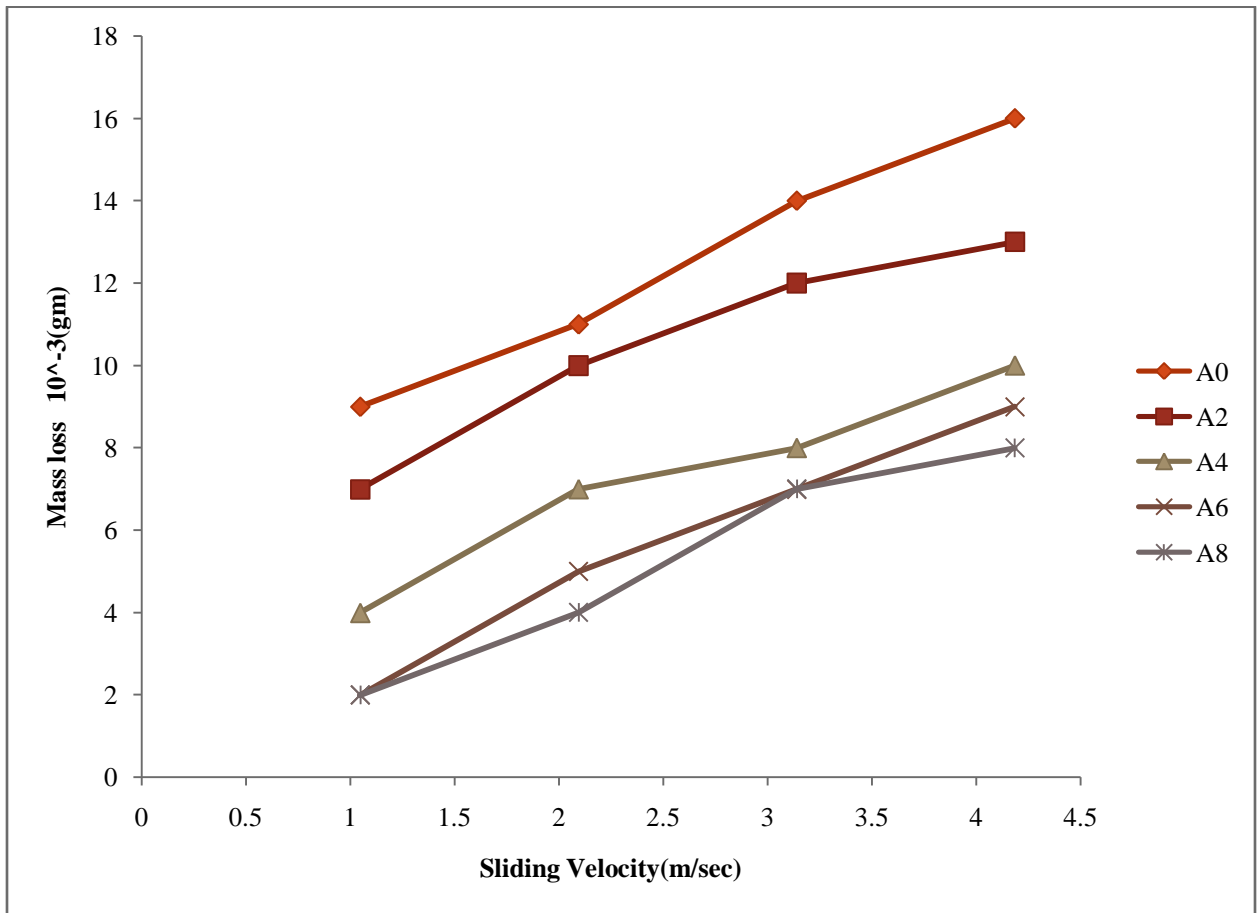


Figure 37 : Wear loss(mass loss) under steady load with variation in sliding velocity

4.10.1 Effect of reinforcement on Wear loss(mass loss) under steady velocity with variation in Load

In figure it has been shown that there is increase in mass loss with increase in the load but increasing the amount of particulate filler content of graphite and flyash leads to decrease in wear loss of the C93700 alloy composite .For A0 with increase in load the wear loss increases and it is maximum for the greatest load which is applied in the experiment .For A2 and A4 also wear loss increase with increase in load but for A4 the increase is less in comparison to A2 due to more amount of graphite and filler content which leads to decrease in value of μ and due to this there is less wear loss for A4.For A6 and A8 there is slight decrease in the wear loss with increase in the load from 15 N to 35 N this can be explained as with increase in load in A6 and A8 there is more graphite and flyash precipitate which come over the surface and thus it leads to decrease in the mass loss due to self lubricating nature of the graphite and smooth surface of the flyash which lead to decrease in the value of μ and it causes less mass loss during application of load.Further increase in the Load leads to more mass loss but mass loss for A8 is least due to maximum content of flyash and graphite particulate in C93700 alloy composite.

M. Kestursatya et al.(76) studied the Wear performance of copper graphite composite and a leaded copper alloy and he founded that Mutual material transfer between the pin and the disk was observed in both CG-steel and LC-steel tribocouples. With increase in the applied load the amount of material transfer from the pin to the surface of the disk increased for both LC and CG materials. However incase of LC-steel tribocouple transfer was observed primarily from the pin to the steel disk, the material transfer included the transfer of lead from the LC pin to the disk. delamination in centrifugally cast C90300/10%graphite composite.

Load	A0	A2	A4	A6	A8
5	.004	.008	.002	.001	.001
15	.009	.007	.006	.005	.003
25	.011	.010	.008	.004	.003
35	.015	.013	.010	.006	.005
45	.018	.016	.012	.009	.008

Table 19 : Wear loss (mass loss) under steady velocity with variation in Load

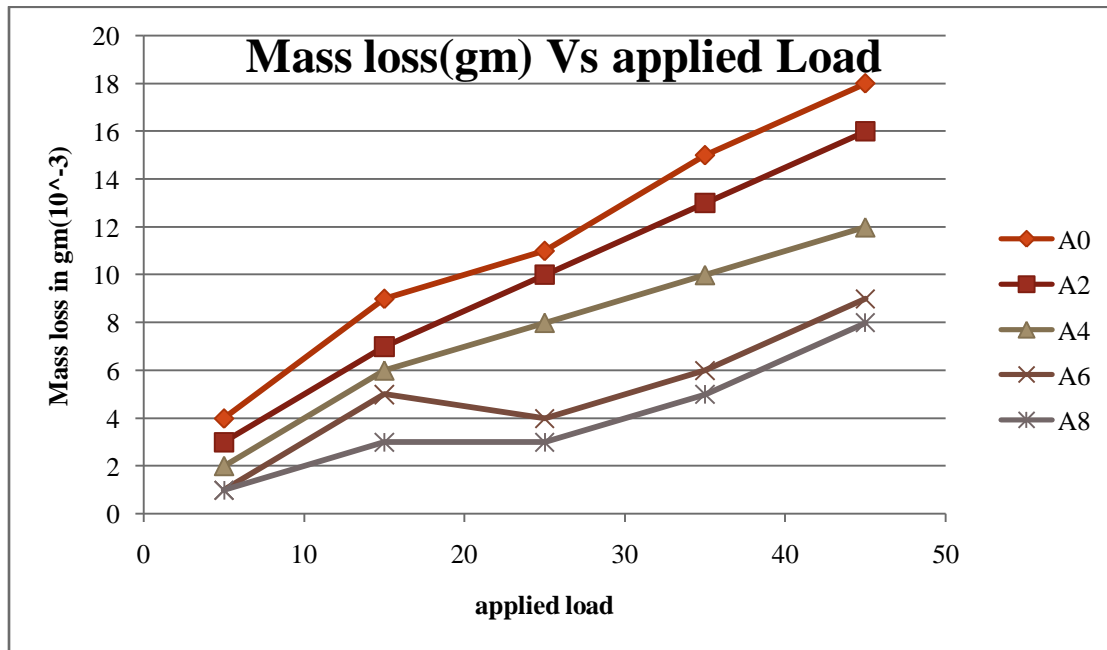


Figure 38 : Wear loss(mass loss) under steady velocity with variation in Load

Chapter Summery

This chapter briefly explains different experimental test conducted on graphite and flyash filled C93700 metal matrix composites. Different mechanical property of the composites has been obtained through various equipments and analysis of property of different samples having different composition of flyash and graphite is investigated.

The next chapter presents the analysis of surface morphology of particulate filled metal alloy composites and optimization of wear rate using taguchi analysis

Chapter 5: ANALYSIS OF SURFACE MORPHOLOGY OF PARTICULATE FILLED METAL ALLOY COMPOSITES AND OPTIMIZATION OF WEAR RATE USING TAGUCHI ANALYSIS

5.1 Surface morphology and wear analysis of particulate filled metal alloy composites

The surface morphology of the alloy composites are observed by Scanning electron microscope. The surfaces appear very less smooth but homogeneous in nature with some submicron pits and cracks due to less amount of residual compressive stresses.. These stresses occurred because of several chemical reactions which occur during drying, and also the significant difference in thermal expansion coefficients between the matrix and the dual reinforcement [80].. The graphite and flyash filled C93700 alloy composites are examined by scanning electron microscopy in order to understand the behavior of void content on tensile strength of the composites. From the Figure 15 it is found that for 0 wt.-% Flyash and graphite filled C93700 alloy composites, void content is more i.e. 3.03wt % as compared to other wt.-% of Flyash and graphite filler. Therefore, through the experimental results, it is found that the void content decreases with increasing wt.-% of Flyash and graphite filler in C93700 alloy composites (Figure 15). For 2024 aluminum alloy metal matrix composites with Al_2O_3 filler particles, the density of the composites increases with size of the particle and with the increase in wt% of the particulate filler, whereas the porosity of the composites increased with decreasing size and increasing weight percentage of particles [81]. Hence, with the decrease in void content the interfacial bonding between the particles of composite is increased and so that it improves the tensile strength of the composites (Figure 22). Otherwise, when void contents remain more, then the strength of the composites will decrease. From the (Figure 35) it is found that the interface bonding between the particles is more adequate and hence the void contents is less and it directly affects the mechanical properties of composites. Similarly, Figure 36 shows more homogeneous composition and thus have less voids (Figure 14) due to increase in graphite and flyash filler materials in the alloy composites. The decrease in voids and due to homogeneity of Composite the

fracture toughness of the composites automatically increases and hence the internal crack propagation taking place is less while performing fracture test.

Scanning electron microscopic investigation was performed on the abraded surfaces. The morphology appears rough and homogeneous with some submicron pores and cracks due to small residual compressive stresses induced during wear. These stresses caused by chemical reactions during drying, and also the difference in thermal expansion coefficients between the substrate and the Flyash and graphite films [77]. During the crystallization large compressive stresses are induced in the material. The densification mainly depend on the particle size. Finer particle results in more densification due to better solubility inside the matrix. The eroded surfaces of graphite and flyash filled C93700 alloy composites are examined by scanning electron microscopy in order to understand the sliding wear mechanisms and characteristic features of wear under steady state condition of velocity and load. The eroded surfaces are observed to be smooth at low sliding velocity for 0wt.-% Flyash and graphite filler in the C93700 alloy composites where it's found higher abraded surface at 4.086 m/sec sliding velocity at constant load of 15N which is shown in Table 18. However, with respect to constant velocity the maximum wear rate is found at the load of 45N for 0wt.-% Flyash and graphite filler in the C93700 alloy composite at constant (1.047m/sec) sliding velocity (Figure 31). With increase the wt.-% of Flyash and graphite (From 0-2, 2-4, 4-6 and 6-8 wt.-%) in C93700 alloy composites it is found that the higher sliding wear or maximum removal of material occurred at higher sliding velocity i.e. 4.186 m/sec. Which are shown by respective figures i.e. 30(A0, A2, A4, A8, A8). Similarly with load the maximum wear is found higher at highest load, for different composition of Flyash and graphite filler in C93700 alloy composites. With the increasing wt.-% of Flyash and graphite filler in C93700 alloy composites the sliding wear or the smoothness of metal will also increase with respect to variation in load and velocity which are shown by different SEM graphs. It is observed through SEM images that for A8 and A6 the precipitation of graphite and flyash is more over the surface which lead to decrease in the wear loss comparatively to A0, A2 and A4.

SEM images

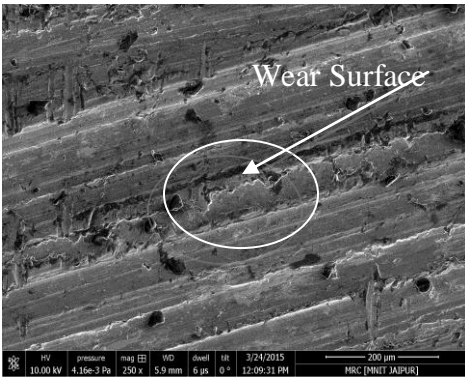


Figure 39: SEM images of 0wt% dual reinforcement

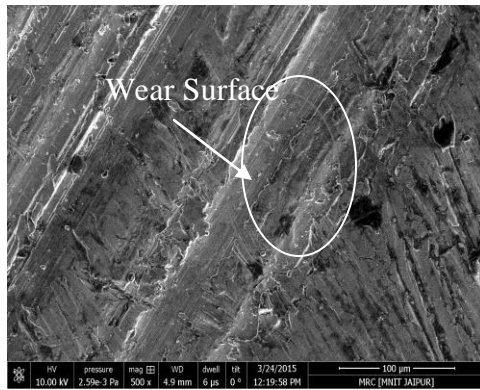


Figure 40: SEM images of 2 wt% dual reinforcement



Figure 41: SEM images of 4 wt% dual reinforcement

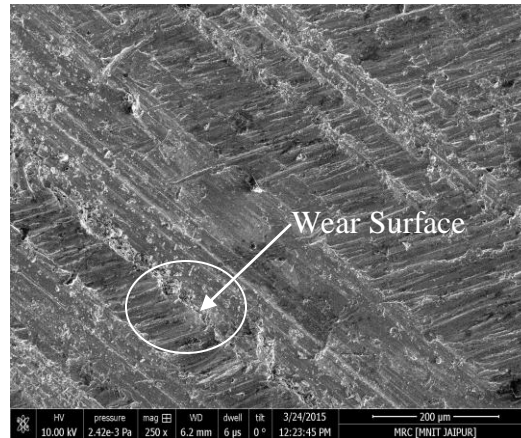


Figure 42: SEM images of 6 wt% dual reinforcement

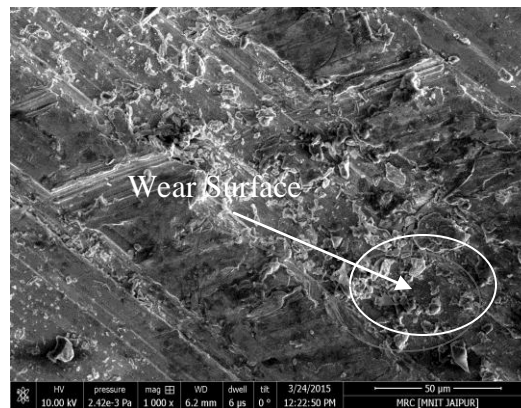


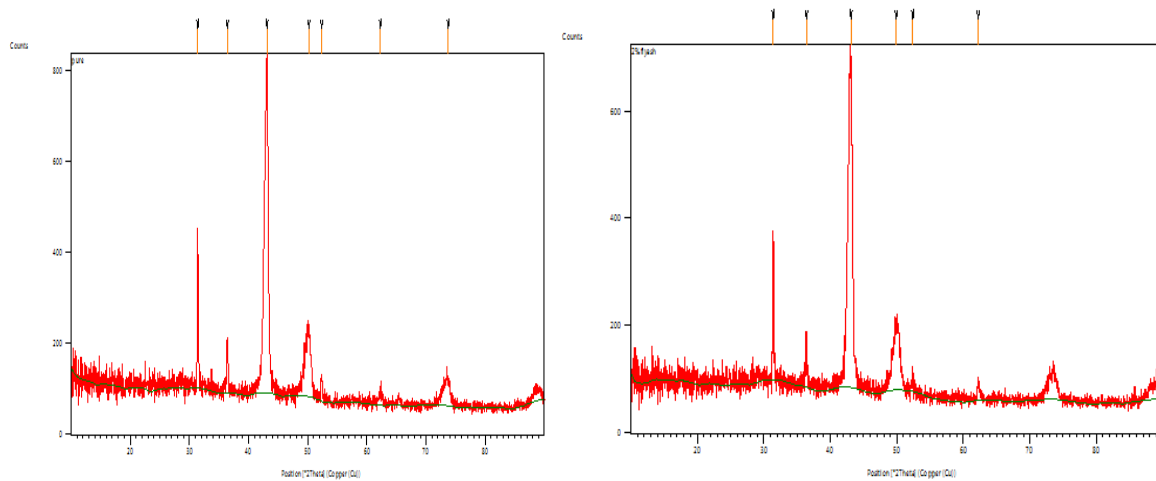
Figure 43: SEM images of 8 wt% dual reinforcement

However, on increase in sliding velocity the abraded surface of the particulate filled alloy matrix composite at constant Load of 15N represents a higher degree of flake formation under high sliding velocity conditions. The formation of flake occurred due to repeated action of Wear particles at a higher impact velocity and ultimately the surface suffered plastic deformation and a work-hardened layer was produced on the surface. Similarly, under similar sliding velocity for other wt.-% Flyash and graphite filled C93700 alloy composites with similar operating conditions the wear increases but loss is due to rubbing of particles on the composite surface under lower load. As the amount of reinforcing graphite and flyash increases in the base material the extent of deformation increases gradually with the increase in sliding Velocity but the rate of increment is less for the composite having higher amount of graphite and flyash in it. The

decrease in the wear rate is due to decrease in the coefficient of friction due to very good self lubrication of the graphite and soft nature of the flyash accompanied by ball bearing effect which is induced due to addition of the flyash.

5.2 Effect of XRD on different filler content

The X-ray diffraction is just the projection of the material and it can also tell about the phase structure of the material with the help of miller indices. Different peaks shows the varying wt% of material and crystal structure of the material can be easily indicated for various types of samples which may be in powder or solid form. It can also identify the nature of different types of polycrystalline phases.



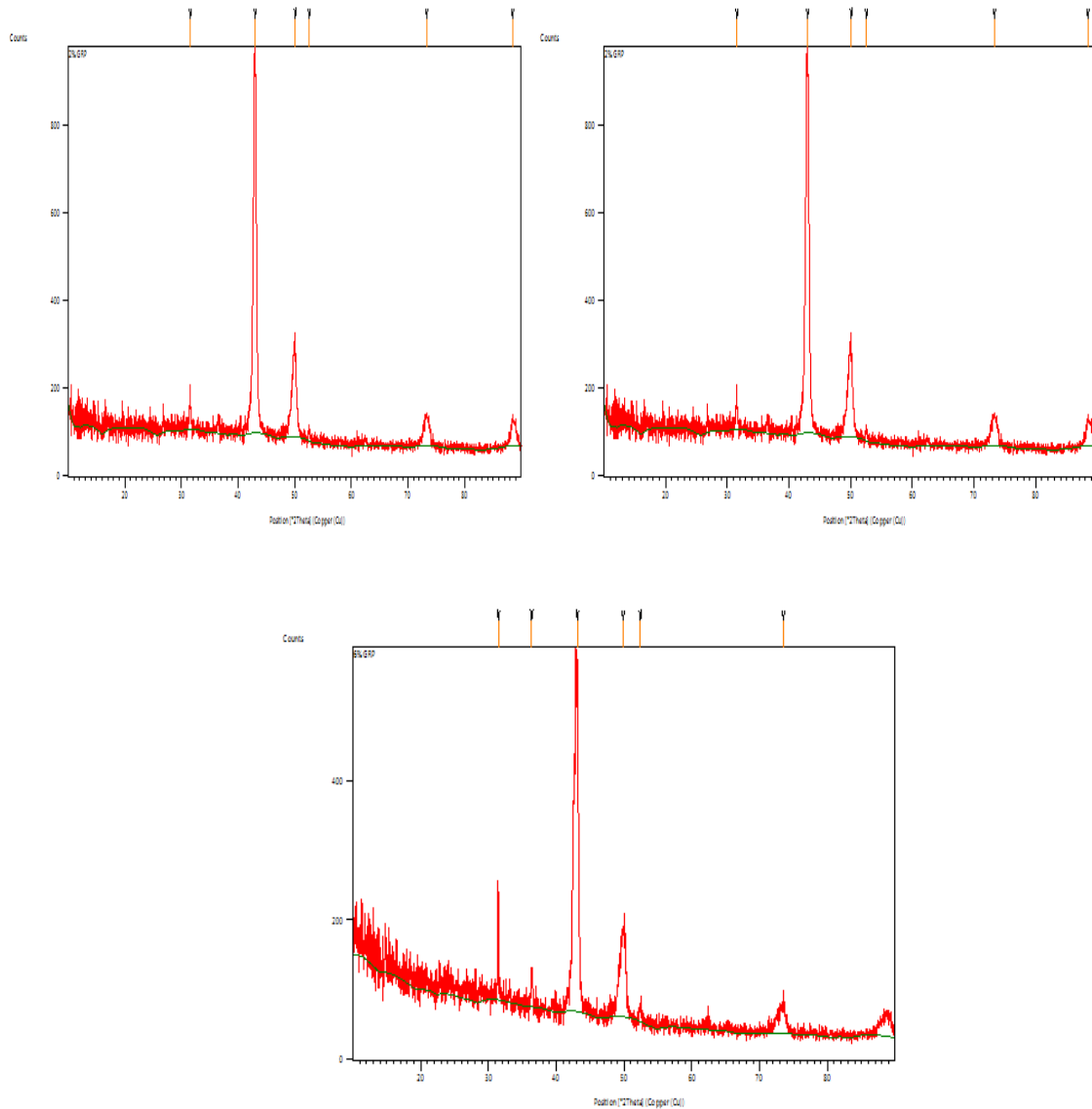


Figure 44 XRD images of different samples of composites

Figure shows the X-ray diffraction pattern for all composition of flyash and graphite filled C93700 alloy composites and the maximum intensity of diffraction peak changes at different 2θ . Figure 4.23 represents the different peaks for different compositions (0wt.-%, 2wt.-%, 4wt.-%, 6wt.-% and 8wt.-%) of Flyash and graphite filled C93700 alloy composites. All composition peaks are shown by different figures. For 0 wt.-%

compositions, the highest peak is found to be at 43.0948° position, similarly for 2 wt.-% and 4 wt.-%, it's found at 43.1181 and 43.0073° respectively and similarly for 6 wt.-% it's found to be at 43.0834° . In the Figure 37 all compositions of Flyash and graphite filled C93700 alloy composites have different peaks at different heights which shows the presence of different composition of different materials in the given composites. The highest peak shows the presence of copper because in the composite the percentage of copper is much more than the other materials. Similarly other peaks show the other material in descending order. . Solís [83] studied the diffraction peaks pattern for commercial Flyash and graphite

The intensity and full width of the diffraction lines shows the high crystallinity of the material. The diffraction patterns of X-Ray diffraction (XRD) reveal the influence of varying weight percentage of flyash and graphite. Comparisons of the mechanical properties are also being made on the unreinforced lead tin bronze matrix (0 wt. %). The compatibility between matrix and reinforcement was indicated from the microstructure examination showing homogeneous distribution of graphite and flyash particles in the alloy matrix . It observed by Nasar [84] that the observation of the maximum intensity diffraction peak at $2\theta = 21.8$ corresponding to d spacing 4.4801\AA , indicating the presence of a typical semi crystalline structure, consistent with earlier studies. X ray diffraction patterns PVA/ Na₂SO₄ (2%, 4%, 6%, 8 % and 10 %) composite system. The XRD pattern of the pure PVA has indicated the presence of crystalline behaviour, in agreement with the results reported earlier. Figure 44 shows X-ray diffraction pattern for all composition of Flyash and graphite filled C93700 alloy composites. In this different peaks are at a certain positions which shows the different materials position and for different peaks for the different compositions (0wt.-%, 2wt.-%, 4wt.-%, 6wt.-% and 8wt.-%). All composition peaks are shown by different colors. For 0wt.-% composition the highest peak found at 43.0948 position. similarly for 2wt.-% and 4wt.-% it is found at 43.1181 , 43.0073° respectively and similarly for 6wt.-% and 8wt.-% it is found 43.0834° and 43.0948° . In Figure 37 all the compositions of Flyash and graphite filled C93700 alloy composites have different peaks at different heights which shows the presence of different composition of different materials in the given composites. The highest peak shows the

presence of Copper because in the composite the percentage of Copper is much more than the other materials. Similarly, other peaks show the other material in descending order. Lee [85] studied the XRD patterns for the transverse cross-sectional plane of the friction stir processed composites. Yar [94] studied about aluminum alloy (A356.1) matrix composites reinforced with 1.5, 2.5 and 5 vol% MgO particle which were fabricated via stir casting method and the phases of material were identified by XRD analysis were similar for all composites. Although, their peak intensity was different but magnesium oxide (MgO), silicon (Si) and aluminum (Al) were just detected and observed that the XRD pattern of composite, containing 1.5 vol.% MgO, fabricated at 850 °C. Similarly, the XRD results showed by the Motlagh [105] that the presence of the Al₇Cu₄Ni phase, white elongated particles which contain Al, Cu and Ni elements based on their EDS analysis. On the other hand, the morphology of the Al₇Cu₄Ni phase is irregular (elongated particles or skeletonlike).

5.2.1 EDS ANALYSIS OF SAMPLES

EDS analysis is one of the vital analysis required to certain about the various types of the compounds present in the sample. Here the EDS is performed to examine the various types of elements presents in the C93700 alloy composite. EDS shows presence of Copper (Cu), Lead (Pb), Tin (Sn) and carbon which is being added to the material in the form of flyash and graphite. EDS analysis signifies that the particulate present in the samples are uniformly distributes as with the increase in dual reinforcement % within the matrix the homogeneity and particulate filler increases inside the C93700 alloy matrix.

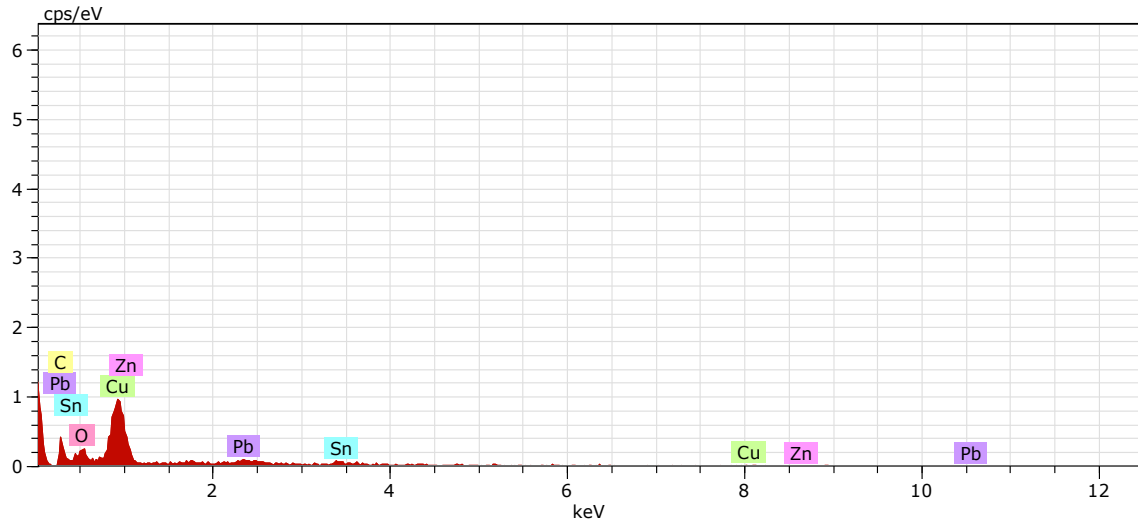


Figure 45 EDS of 8% dual Reinforced C93700 alloy matrix

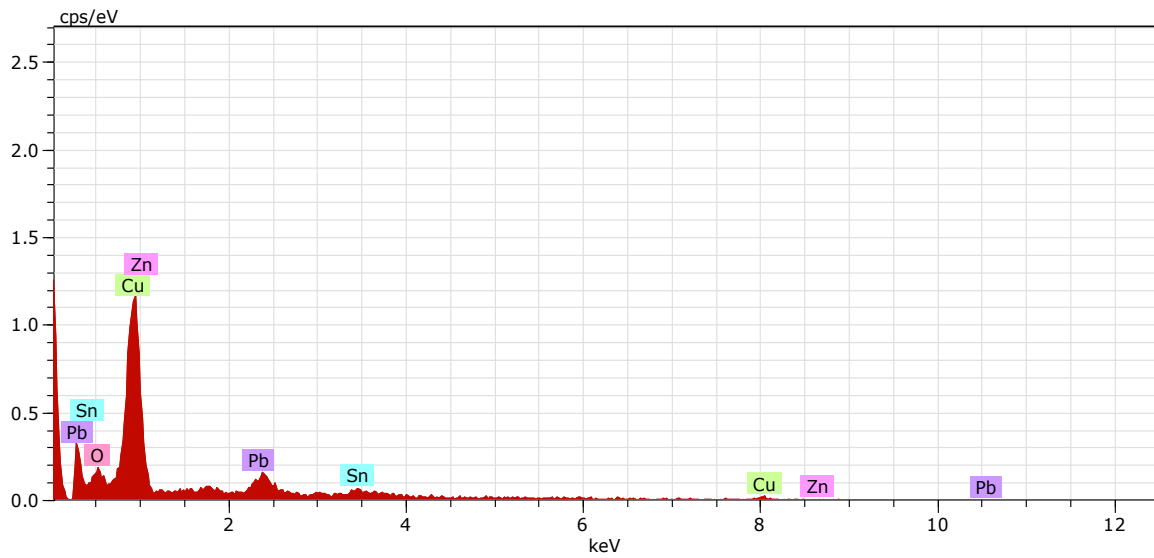


Figure 46 EDS of 6% dual Reinforced C93700 alloy matrix

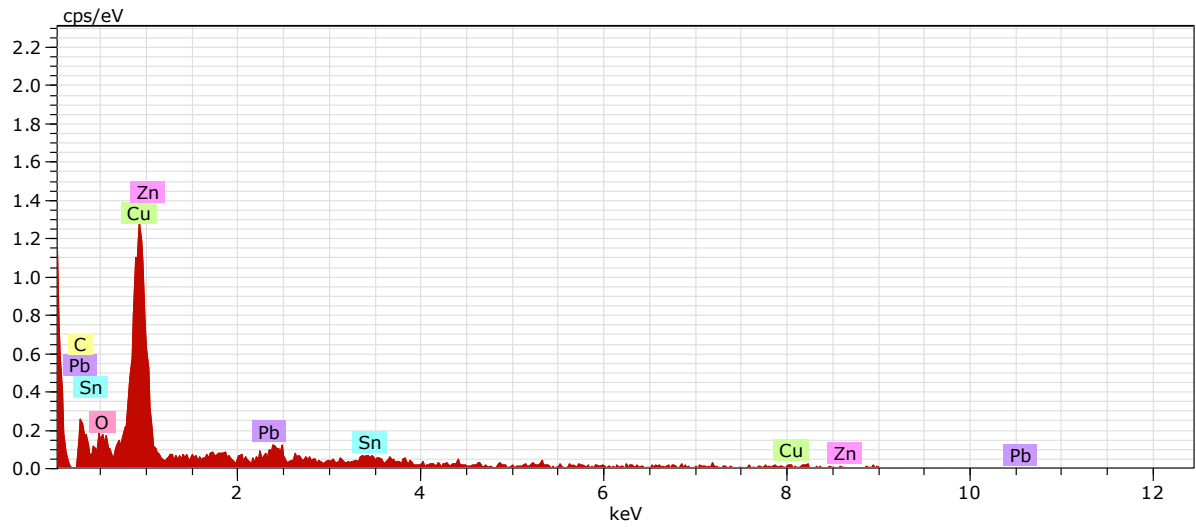


Figure 47 EDS of 4% dual Reinforced C93700 alloy matrix

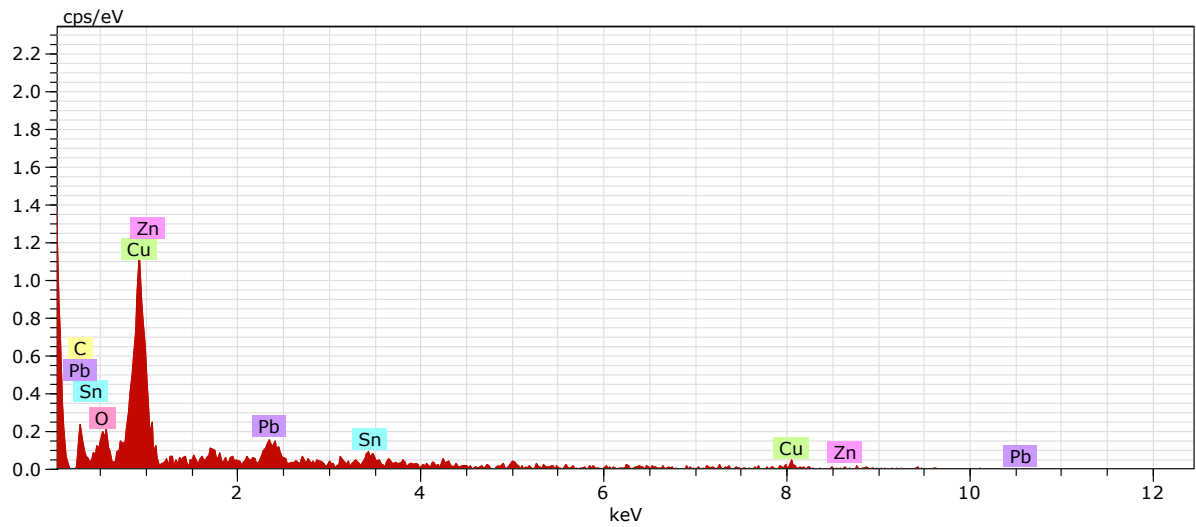


Figure 48 EDS of 2% dual Reinforced C93700 alloy matrix

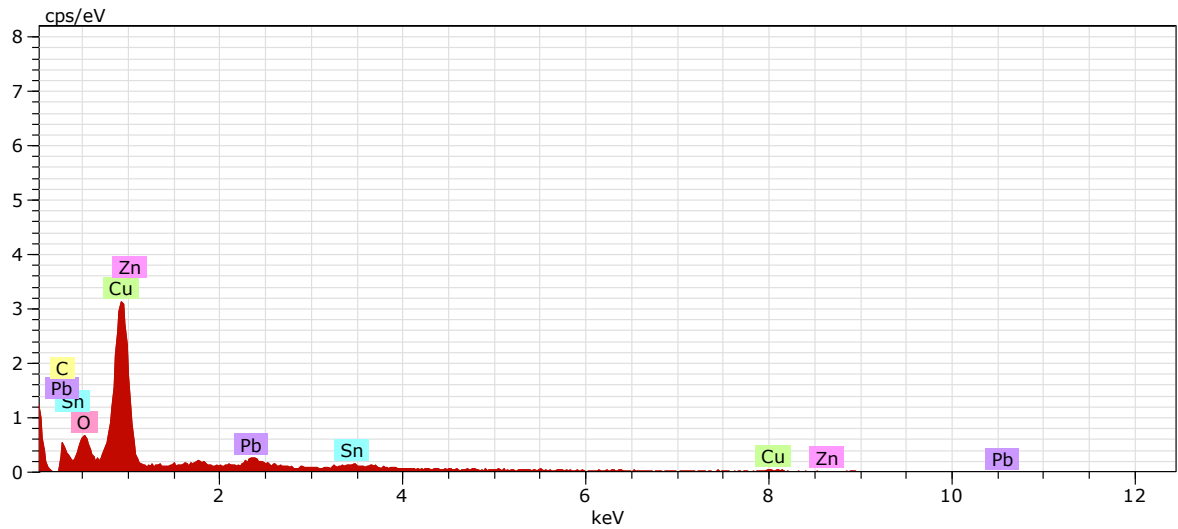


Figure 49 EDS of Pure C93700 Alloy

5.3 Optimization of wear rate factor by taguchi method

Taguchi's method for experimental design is straight forward and easy to apply to many engineering situations, making it a powerful yet simple tool. It can be used to quickly narrow down the scope of a research project or to identify problems in a manufacturing process from data already in existence. Also, the Taguchi method allows for the analysis of many different parameters without a prohibitively high amount of experimentation. In Table 20, the eight columns represents S/N ratio of the wear rate which can be considered as fingerprint of average of different factor of composite.

Table 20 : Experimental design using L_{25} orthogonal array (Graphite and flyash filled)

Sl.no	Reinforcement	Sliding velocity	load	Sliding distance	Wear rate(gm/gm)	density	S/N ratio (db)	Mean
	A0	1.047	5	942.3	0.004	8.591	47.9588	0.004
	A0	2.094	15	1884.6	0.006	8.591	44.43697	0.006
	A0	3.14	25	2826	0.01	8.591	40	0.01
	A0	4.186	35	3767.4	0.014	8.591	37.07744	0.014
	A0	5.233	45	4709.7	0.019	8.591	34.42493	0.019
	A2	1.047	15	2826	0.007	8.588	43.09804	0.007
	A2	2.094	25	3767.4	0.011	8.588	39.17215	0.011

	A2	3.14	45	4709.7	0.016	8.588	35.9176	0.016
	A2	4.186	15	942.3	0.013	8.588	37.72113	0.013
	A2	5.233	5	1884.6	0.009	8.588	40.91515	0.009
	A4	1.047	25	4709.7	0.008	8.576	41.9382	0.008
	A4	2.094	35	942.3	0.012	8.576	38.41638	0.012
	A4	3.14	45	1884.6	0.015	8.576	36.47817	0.015
	A4	4.186	5	2826	0.007	8.576	43.09804	0.007
	A4	5.233	15	3767.4	0.011	8.576	39.17215	0.011
	A6	1.047	35	1884.6	0.013	8.527	37.72113	0.013
	A6	2.094	45	2826	0.017	8.527	35.39102	0.017
	A6	3.14	5	3767.4	0.012	8.527	38.41638	0.012
	A6	4.186	15	4709.7	0.014	8.527	37.07744	0.014
	A6	5.233	25	942.3	0.016	8.527	35.9176	0.016
	A8	1.047	45	3767.4	0.009	8.486	40.91515	0.009
	A8	2.094	5	4709.7	0.002	8.486	53.9794	0.002
	A8	3.14	15	1884.6	0.005	8.486	46.0206	0.005
	A8	4.186	25	2826	0.008	8.486	41.9382	0.008
	A8	5.233	35	3767.4	0.01	8.486	40	0.01

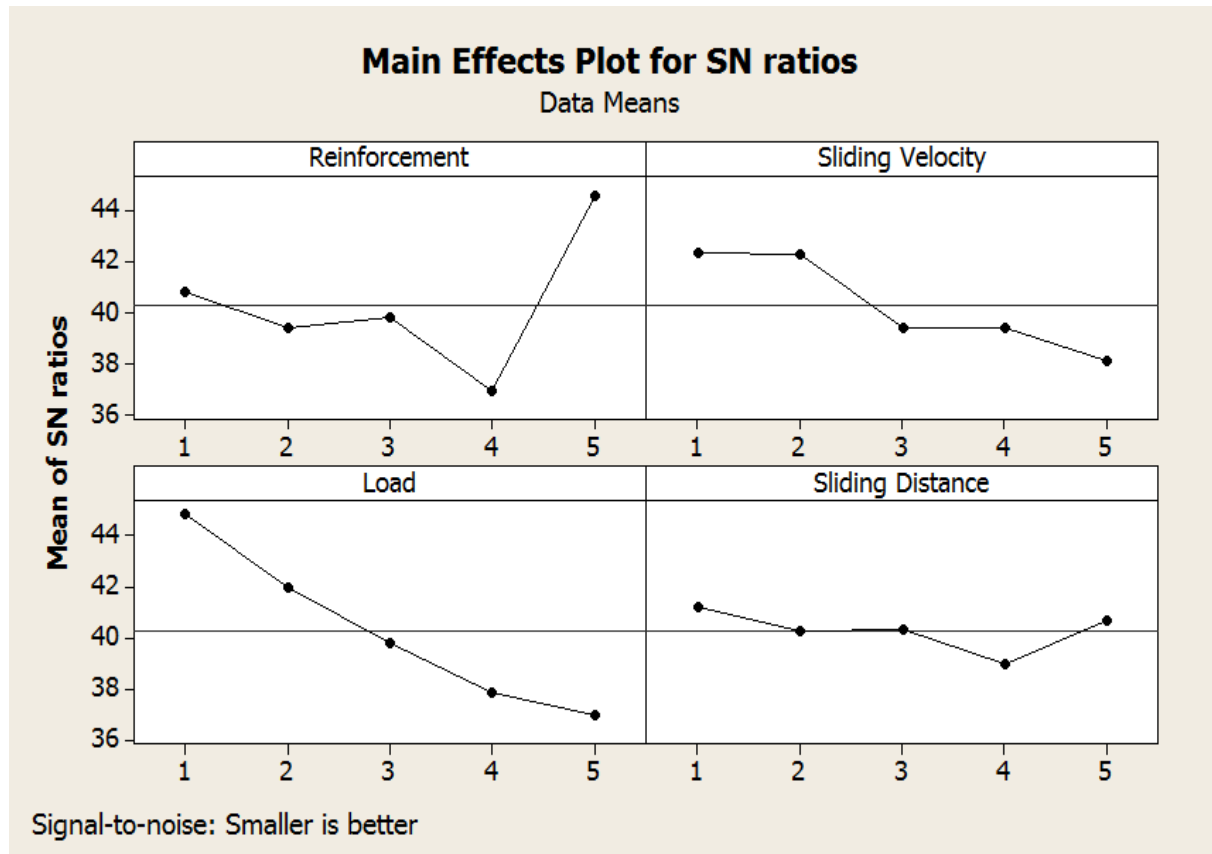


Figure 50 Graph Showing the Effect of different factor on wear rate

The overall mean for the S/N ratio of the wear rate is found to be 39.56 db. The Analysis was performed with the powerful statistical tool MINITAB 16 which is capable of producing effect of controlled factor and can lead to elimination of least significant parameter. The dependence of various Controlled factor must be analyzed with the wear rate and the best factors must be selected. Thus factorial design incorporates a simple means of testing for the presence of the interaction effects. Analysis of the result leads to the conclusion that factor combination of A,B, C, D which are reinforcement, sliding velocity, load and sliding distance respectively and taguchi analysis shows that reinforcement is the 2nd most important factor in minimizing the wear rate and graphite and flyash filled composite gives minimum wear rate for C93700 metal matrix composites (figure 38). This analysis establishes that wear rate also depends upon the types of filler, sliding velocity and sliding distance.

5.4. ANOVA for graphite and flyash filled C93700 alloy composites

The ANOVA is used to analyze the influence of various wear parameters like sliding velocity, filler content, sliding Distance and load to analyze their tribological performance on wear rate.

Table 21 describe the various controlled factor of ANOVA analysis. It can be observed from the ANOVA analysis (Table 21) that the sliding velocity, dual reinforcement content, load and sliding Distance has the influence on wear rate of the composite. The last column of the Table 21 shown indicates the percentage contribution (p) of each factor on the total variation indicating their degree of influence on the result. It can be observed from the ANOVA table that the reinforcement content (p=.002), sliding velocity (p = .017), Load (p = .001) have great influence on the Wear rate. The sliding Distance(.418) shows not much significant effect on wear rate in comparison to other parameters.

Table 21.ANOVA table for wear rate (Graphite and Flyash filled)

Source	DF	Seq SS	Adj SS	Adj MS	F	P
A	4	155.50	155.50	38.875	12.35	.002
B	4	73.19	73.19	18.297	5.81	.017
C	4	205.16	205.16	51.291	16.29	.001
D	4	13.89	13.89	3.472	1.10	.418
Residual Error	8	25.18	25.18	3.148		
Total	24					

DF: degree of freedom, Seq SS: sequential sum of squares, Adj. SS: extra sum of squares, Seq MS: sequential mean squares,F: F-test, %P percent contribution.

5.5 Factor settings for minimum Wear rate

During the study of Wear rate the main focus was to investigate the optimal setting of the various control factor for reducing the wear rate. The objective was to develop a relationship between several control factor with the wear rate.

In order to express, Wear rate in terms of mathematical model in the following form is suggested.

$$W_r = K_0 + k_1 \times A + K_2 \times B + K_3 \times C + K_4 \times D$$

Here, W_r indicates the performance of several factor with wear rate and K_i ($i = 0, \dots, 4$) are the model constants. The constant are calculated using non-linear regression analysis the following relations are obtained.

$$C_5 = 0.00124 - 0.000440 A + 0.00112 B + 0.00200 C + 0.000480 D \quad r^2 = 0.87$$

The correctness of the obtained constants is verified as high correlation coefficients (r^2) in the range of 0.87 are obtained from the above mentioned equation and therefore, the models are quite suitable and can be use for further Analysis.

Table 22: Response Table for Signal to Noise Ratios

Smaller is better

Level	A	B	C	D
1	40.78	42.33	44.87	41.21
2	39.36	42.28	41.96	40.30
3	39.82	39.37	39.79	40.32
4	36.90	39.38	37.83	38.95
5	44.57	38.09	36.99	40.67
Delta	7.67	4.24	7.89	2.26
Rank	2	3	1	4

Where A=Reinforcement, B=Sliding Velocity, C=Load, D= Sliding Distance

Chapter Summary

This chapter has provided:

- The experimental results sliding wear tests for fly ash and graphite particulates filled C93700 alloy composites.
- The comparison of different wt% of particulate fillers with regard to the steady state sliding Wear performance of composites under similar test conditions.
- The analysis of the experimental results using Taguchi method.

- The surface morphologies of abraded composites using scanning electron microscope
- EDS characterizations of all the particulate filled alloy composites have done and the composition of different wt % of flyash and graphite reinforced fillers and alloy materials was identified using EDS.

The next chapter presents the summary of research findings and conclusions drawn from this investigation along with recommendations for potential applications and future work.

Chapter 6: SUMMARY AND CONCLUSIONS

This chapter presents the comparative analysis of graphite and flyash particulate filled C93700 alloy composites systematically. The proposed particulate filled alloy composites show quite different physical, mechanical and fracture toughness than alloy composites.

6.1 Effect on Void Content with the Addition of Graphite and Flyash particulate in C93700 alloy matrix

It is observed that the flyash and graphite particulate reinforcement has less void content as compared to only graphite particulate filled composites. This behavior of void content may show the good adhesion between reinforcement and matrix material. It is given in literatures that the void content lowers the quality of product, affects various properties and may cause pre-mature failure while in servicing/functioning [77]. However, the void fraction should be as minimum as possible, in this case we can't neglect the said voids and the void fraction in the said composites is acceptable.

6.2 Effect on Hardness with the Addition of Graphite and Flyash particulate in C93700 alloy matrix

The hardness of the composites increases with the increment in wt.-% of filler up to 2% and then it gradually decreases on increasing the content of graphite keeping the wt.-% of flyash constant in each sample. The hardness of the graphite and flyash filled alloy composites decreases with increasing the amount of the dual filler contents. It is expected that the hardness is dependent on grain size of matrix by following Hall-Patch equation [77]. The decrease in hardness is also attributable to the soft graphite and flyash particles acting as weak barriers to the movement of dislocations within the matrix [78].

6.3 Effect on Tensile Strength with the Addition of Graphite and Flyash particulate in C93700 alloy matrix

The tensile test performed on the samples shows that increasing the amount of graphite filled in the metal matrix keeping the amount of flyash constant (wt%=2) increases the tensile

strength of the material upto(wt%=6) but after that increasing the amount of graphite results in the decrement in the value of tensile strength.

6.4 Effect on Impact Strength with the Addition of Graphite and Flyash particulate in C93700 alloy matrix

The impact strength is increased with the increasing in reinforcement upto (4%) weight percentages further increase in the amount of the dual reinforcement results in the decrease in the value of the Impact strength.

6.5 Effect On Ductility with the Addition of Graphite and Flyash particulate in C93700 alloy matrix

As the content of graphite and flyash increases, the ductility of the composite material increases by considerable amounts, i.e., when the graphite content is increased from 0% to 8 % the ductility was found to increase by about 163% and further increment in the content of flyash and graphite leads to further increase in the elongation %.

6.6 Effect on Compression Strength with the Addition of Graphite and Flyash particulate in C93700 alloy matrix

It has been observed that addition of flyash and graphite in C93700 alloy composite leads to increase in the compressive strength of the material. Increase in Compressive strength can be attributed as better bonding between particulate and C93700 alloy matrix.

6.7 Effect on Flexural Strength with the Addition of Graphite and Flyash particulate in C93700 alloy matrix

The flexural strength increases with the increase in flyash and graphite particulate filled alloy composites. The flexural strength of the specimens increases with increase in addition of filler but it has been found that the flexure strength increase gradually upto 6% but further addition results in very small increase in the flexural strength of the composite

6.8 Effect on Coefficient of Friction (μ) with the Addition of Graphite and Flyash particulate in C93700 alloy matrix

Increase in amount of the graphite and flyash in C93700 alloy matrix leads to decrease in the value of μ . Though it is found that with increase in the sliding velocity the coefficient of friction reduces but the decrease is maximum for the 4% (graphite and flyash) filler content. It has been observed that increase in the amount of reinforcement leads to decrease in the coefficient of friction but it has been found that there is gradual increase in the coefficient of friction for

6.9 Effect on Wear rate with the Addition of Graphite and Flyash particulate in C93700 alloy matrix

It has been found that there is increase in mass loss with increase in the load but increasing the amount of particulate filler content of graphite and flyash leads to decrease in wear loss of the C93700 alloy composite. It is observed that decrease in the mass loss due to self lubricating nature of the graphite and smooth surface of the flyash which lead to decrease in the value of μ and it causes less mass loss during pressure of load. Further increase in the Load leads to more mass loss but mass loss for A8 (maximum content of graphite having 2% flyash) is least due to maximum content of flyash and graphite particulate in C93700 alloy composite.

6.10 Scope for future work

Through the stages of project development several important observations were made which will require additional investigation and research. The following can be considered as a part of future study and development of new material composite

- There is a great need to have the better control of the grain size, particle size and shape of graphite and flyash fillers in order to enhance the wear properties. Hence, in the future, Graphite and flyash fillers will be synthesized such that there will be adequate control over the reinforcement shape and size.

- Presence of both toughening phase and solid lubricants dispersed in the C93700 matrix results in a favorable combination of tribological properties of metal alloy composites: good wear resistance and low coefficient of friction.
- The present investigation is limited to Vacuum casting only. The other casting techniques could be tried and analyzed so that a final conclusion can be drawn more effectively.
- Cost analysis of these composites to assess their economic viability in industrial applications.

Chapter summery

This chapter comprehensively compares the different results which obtained from the Dual reinforcement of C93700 alloy composite in relation of various properties which discussed in previous chapter.

REFERENCES

- [1] He, Y., Zhao, Z., Luo, T., Lu, X., & Luo, J. (2013). Failure analysis of journal bearing used in turboset of a power plant. *Materials & Design*, 52, 923-931.
- [2] Essential Concepts of Bearing Technology, Fifth Edition By Tedric A. Harris, Michael N. Kotzalas
- [3] Tiwari, M., Gupta, K., & Prakash, O. (2000). Effect of radial internal clearance of a ball bearing on the dynamics of a balanced horizontal rotor. *Journal of sound and vibration*, 238(5), 723-756.
- [4] nptel.ac.in/courses/IIT-MADRAS/Machine_Design_II/pdf/5_1.pdf
- [5] Becker, W. T., Shipley, R. J., Lampman, S. R., Sanders, B. R., Anton, G. J., Hrivnak, N., ... & Scott Jr, W. W. (2002). *ASM handbook. Failure analysis and prevention*, 11.
- [6] Woydt, M., & Wäsche, R. (2010). The history of the Stribeck curve and ball bearing steels: The role of Adolf Martens. *Wear*, 268(11), 1542-1546.
- [7] Kallio M, Vuorinen P, Fuentes E, Marañña O, Ruusila V, Nyssönen T, et al. Tribological behavior of bronze alloys with solid lubricants. *Key Engineering Materials* 2012;527:205-210.
- [8] Equey, S., Houriet, A., & Mischler, S. (2011). Wear and frictional mechanisms of copper-based bearing alloys. *Wear*, 273(1), 9-16.
- [9] Davis, J. R. (Ed.). (2001). *Surface engineering for corrosion and wear resistance*. ASM international.
- [10] Xiao, L., Rosen, B. G., Amini, N., & Nilsson, P. H. (2003). A study on the effect of surface topography on rough friction in roller contact. *Wear*, 254(11), 1162-1169.

- [11] Qu, J., Truhan, J. J., Blau, P. J., & Ott, R. (2007). The development of a “pin-on-twin” scuffing test to evaluate materials for heavy-duty diesel fuel injectors. *Tribology Transactions*, 50(1), 50-57.
- [12] Blau, P. J. (2001). The significance and use of the friction coefficient. *Tribology International*, 34(9), 585-591
- [13] Davis, J. R. (Ed.). (2001). *Surface engineering for corrosion and wear resistance*. ASM international.
- [14] Szeri, A. Z. (2010). *Fluid film lubrication*. Cambridge University Press.
- [15] Lundberg, J. (1995). Influence of surface roughness on normal-sliding lubrication. *Tribology international*, 28(5), 317-322.
- [16] Pattabhiraman S, Levesque G, Kim NH, Arakere NK. " Uncertainty analysis for rolling contact fatigue failure probability of silicon nitride ball bearings. *International Journal of Solids and Structures* 2010;47:2543–53
- [17] Becker, W. T., Shipley, R. J., Lampman, S. R., Sanders, B. R., Anton, G. J., Hrivnak, N., ... & Scott Jr, W. W. (2002). *ASM handbook. Failure analysis and prevention*, 11.
- [18] Upadhyay, R. K., L. A. Kumaraswamidhas, and Md Sikandar Azam. "Rolling element bearing failure analysis: A case study." *Case Studies in Engineering Failure Analysis* 1.1 (2013): 15-17
- [19] Tauqir, A., et al. "Causes of fatigue failure in the main bearing of an aero-engine." *Engineering Failure Analysis* 7.2 (2000): 127-144.
- [20] Muzakkir, S. M., et al. "Tribological failure analysis of journal bearings used in sugar mills." *Engineering Failure Analysis* 18.8 (2011): 2093-2103
- [21] Gurumoorthy, K., and Arindam Ghosh. "Failure investigation of a taper roller bearing: A case study." *Case Studies in Engineering Failure Analysis* 1.2 (2013): 110-114

- [22] Singla, M., Dwivedi, D. D., Singh, L., & Chawla, V. (2009). Development of aluminium based silicon carbide particulate metal matrix composite. *Journal of Minerals and Materials Characterization and Engineering*, 8(06), 455.
- [23] T.W.Clyne, *Metal Matrix Composites: Matrices and Processing*, Encyclopedia of Materials: Science and Technology 2001
- [24] Sharma, S. C., Girish, B. M., Kamath, R., & Satish, B. M. (1997). Effect of SiC particle reinforcement on the unlubricated sliding wear behaviour of ZA-27 alloy composites. *Wear*, 213(1), 33-40.
- [25] B.G. Park, A.G. Crosky, A.K. Heller. Material characterization and mechanical properties of Al₂O₃-Al metal matrix composites. *Journal of materials science* 2001; 36:2417-2426.
- [26] P.Poza,J.Llorca, Mechanical behavior of AL-Li-SiC Composites: Part 1. Microstructure and tensile deformation, *Metallurgical and Materials transactions A*,30;1999:845;855
- [27]CG Cordovilla, J Narciso, E Louis. Abrasive Wear Resistance of Aluminum Alloy/Ceramic Particulate Composites [J]. *Wear*, 1996, 192: 170-177
- [28] Rajkumar, K., & Aravindan, S. (2011). Tribological performance of microwave sintered copper–TiC–graphite hybrid composites. *Tribology International*, 44(4), 347-358.
- [29] Prieto, R., Molina, J. M., Narciso, J., & Louis, E. (2011). Thermal conductivity of graphite flakes–SiC particles/metal composites. *Composites Part A: Applied Science and Manufacturing*, 42(12), 1970-1977.
- [30] Cui, G., Bi, Q., Zhu, S., Yang, J., & Liu, W. (2012). Tribological properties of bronze–graphite composites under sea water condition. *Tribology International*, 53, 76-86.

- [31] Sarmadi, H., Kokabi, A. H., & Reihani, S. S. (2013). Friction and wear performance of copper-graphite surface composites fabricated by friction stir processing (FSP). *Wear*, 304(1), 1-12.
- [32] Rajmohan, T., & Palanikumar, K. (2011). Experimental investigation and analysis of thrust force in drilling hybrid metal matrix composites by coated carbide drills. *Materials and Manufacturing Processes*, 26(8), 961-968.
- [33] Kumar, A., Lal, S., & Kumar, S. (2013). Fabrication and characterization of A359/Al 2 O 3 metal matrix composite using electromagnetic stir casting method. *Journal of Materials Research and Technology*, 2(3), 250-254.
- [34] Gopalakrishnan, S., & Murugan, N. (2012). Production and wear characterisation of AA 6061 matrix titanium carbide particulate reinforced composite by enhanced stir casting method. *Composites Part B: Engineering*, 43(2), 302-308.
- [35] Poddar, P., Mukherjee, S., & Sahoo, K. L. (2009). The microstructure and mechanical properties of SiC reinforced magnesium based composites by rheocasting process. *Journal of materials engineering and performance*, 18(7), 849-855.
- [36] Sajjadi, S. A., Ezatpour, H. R., & Parizi, M. T. (2012). Comparison of microstructure and mechanical properties of A356 aluminum alloy/Al 2 O 3 composites fabricated by stir and compo-casting processes. *Materials & Design*, 34, 106-111.
- [37] Mahendra, K. V., & Radhakrishna, K. (2007). Fabrication of Al-4.5% Cu alloy with fly ash metal matrix composites and its characterization. *Materials Science-Poland*, 25(1), 57-68.
- [38] Yu Xiaodong , Wang Yang Wei , and Wang Fu shame (2007). Effect of particle size on mechanical properties of SiC_p/5210 Al metal matrix composite. *Transactions of Nonferrous Metals Society of China*, 1.

- [39] Hemanth, J. (2005). Tribological behavior of cryogenically treated B 4 Cp/Al–12% Si composites. *Wear*, 258(11), 1732-1744.
- [40] Kang, C. G., & Yun, K. S. (1996). Fabrication of metal-matrix composites by the die-casting technique and the evaluation of their mechanical properties. *Journal of materials processing technology*, 62(1), 116-123.
- [41] Milan, M. T., & Bowen, P. (2004). Tensile and fracture toughness properties of SiCp reinforced Al alloys: effects of particle size, particle volume fraction, and matrix strength. *Journal of materials engineering and performance*, 13(6), 775-783.
- [42] Sharma, S. C., Seah, K. H. W., Satish, B. M., & Girish, B. M. (1996). Effect of short glass fibers on the mechanical properties of cast ZA-27 alloy composites. *Materials & Design*, 17(5), 245-250.
- [43] Scudino, S., Liu, G., Sakaliyska, M., Surreddi, K. B., & Eckert, J. (2009). Powder metallurgy of Al-based metal matrix composites reinforced with β -Al 3 Mg 2 intermetallic particles: Analysis and modeling of mechanical properties. *Acta Materialia*, 57(15), 4529-4538.
- [44] Skarvelis, P., & Papadimitriou, G. D. (2009). Microstructural and tribological evaluation of potential self-lubricating coatings with MoS₂ \ MnS additions produced by the plasma transferred arc technique. *Tribology International*, 42(11), 1765-1770.
- [45] Wu, L., Chen, J. X., Liu, M. Y., Bao, Y. W., & Zhou, Y. C. (2009). Reciprocating friction and wear behavior of Ti 3 AlC 2 and Ti 3 AlC 2/Al 2 O 3 composites against AISI52100 bearing steel. *Wear*, 266(1), 158-166.
- [46] Scudino, S., Liu, G., Prashanth, K. G., Bartusch, B., Surreddi, K. B., Murty, B. S., & Eckert, J. (2009). Mechanical properties of Al-based metal matrix composites reinforced with Zr-based glassy particles produced by powder metallurgy. *Acta Materialia*, 57(6), 2029-2039.

- [47] Emamy, M., Khodadadi, M., Raouf, A. H., & Nasiri, N. (2013). The influence of Ni addition and hot-extrusion on the microstructure and tensile properties of Al–15% Mg 2 Si composite. *Materials & Design*, 46, 381-390.
- [48] Lei, T., Tang, W., Cai, S. H., Feng, F. F., & Li, N. F. (2012). On the corrosion behaviour of newly developed biodegradable Mg-based metal matrix composites produced by in situ reaction. *Corrosion Science*, 54, 270-277.
- [49] Bhatt, J., Balachander, N., Shekher, S., Karthikeyan, R., Peshwe, D. R., & Murty, B. S. (2012). Synthesis of nanostructured Al–Mg–SiO₂ metal matrix composites using high-energy ball milling and spark plasma sintering. *Journal of Alloys and Compounds*, 536, S35-S40.
- [50] Chaubey, A. K., Scudino, S., Mukhopadhyay, N. K., Khoshkhoo, M. S., Mishra, B. K., & Eckert, J. (2012). Effect of particle dispersion on the mechanical behavior of Al-based metal matrix composites reinforced with nanocrystalline Al–Ca intermetallics. *Journal of Alloys and Compounds*, 536, S134-S137.
- [51] Tavighi, K., Emamy, M., & Emami, A. R. (2013). Effects of extrusion temperature on the microstructure and tensile properties of Al–16wt% Al₄ Sr metal matrix composite. *Materials & Design*, 46, 598-604.
- [52] Ali, F., Scudino, S., Liu, G., Srivastava, V. C., Mukhopadhyay, N. K., Khoshkhoo, M. S. & Eckert, J. (2012). Modeling the strengthening effect of Al–Cu–Fe quasicrystalline particles in Al-based metal matrix composites. *Journal of Alloys and Compounds*, 536, S130-S133.
- [53] Liu, Y., Zhou, J., & Shen, T. (2013). Effect of nano-metal particles on the fracture toughness of metal–ceramic composite. *Materials & Design*, 45, 67-71.
- [54] Kumar, S., Panwar, R. S., & Pandey, O. P. (2013). Effect of dual reinforced ceramic particles on high temperature tribological properties of aluminum composites. *Ceramics International*, 39(6), 6333-6342.

- [55] Li, J., Liu, Q., Shi, R. X., Wen, Y., & Yin, Y. S. (2008). Preparation and mechanical properties of Fe 3 Al (Ti)/TiC composites. *Journal of materials processing technology*, 208(1), 105-110.
- [56] Srivatsan, T. S., & Prakash, A. (1995). The quasi-static fracture behavior of an aluminum alloy metal-matrix composite. *Composites science and technology*, 54(3), 307-315.
- [57] Srivatsan, T. S., & Vasudevan, V. K. (1998). Cyclic plastic strain response and fracture behavior of 2080 aluminum alloy metal matrix composite. *International journal of fatigue*, 20(3), 187-202.
- [58] Umanath, K., Selvamani, S. T., Natarajan, K., & Palanikumar, K. (2010, November). Influence of silicon carbide particulate reinforcement on the Fracture toughness of Al 6061 alloy composites produced by stir casting method. In *Frontiers in Automobile and Mechanical Engineering (FAME)*, 2010 (pp. 32-37). IEEE.
- [59] Agrawal, P., & Sun, C. T. (2004). Fracture in metal–ceramic composites. *Composites Science and technology*, 64(9), 1167-1178.
- [60] Cannillo, V., Leonelli, C., Manfredini, T., Montorsi, M., Veronesi, P., Minay, E. J., & Boccaccini, A. R. (2005). Mechanical performance and fracture behaviour of glass–matrix composites reinforced with molybdenum particles. *Composites science and technology*, 65(7), 1276-1283.
- [61] G. A. Sargent, P. K. Mehrotra, H. Conrad. Erosion Prevention and Useful Application, ASTM STP 664, In: Adler, W. F. (ed.), American Society for Testing and Materials 1979;77:427-428
- [62] Zhou, J., Drużdżel, A. T., & Duszczyk, J. (1999). The effect of extrusion parameters on the fretting wear resistance of Al-based composites produced via powder metallurgy. *Journal of materials science*, 34(20), 5089-5097.

- [63] Ramesh, C. S., Srinivas, C. K., & Channabasappa, B. H. (2009). Abrasive wear behaviour of laser sintered iron–SiC composites. *Wear*, 267(11), 1777-1783.
- [64] Miyajima, T., & Iwai, Y. (2003). Effects of reinforcements on sliding wear behavior of aluminum matrix composites. *Wear*, 255(1), 606-616.
- [65] Vencel, A., Rac, A., Bobić, I., & Mišković, Z. (2006). Tribological properties of Al-Si alloy A356 reinforced with Al₂O₃ particles. *environment*, 12, 14.
- [66] Asthana, R. (1998). Processing effects on the engineering properties of cast metal-matrix composites. *Advanced Performance Materials*, 5(3), 213-255.
- [67] Jin, Y., Kato, K., & Umehara, N. (1999). Further investigation on the tribological behavior of Al₂O₃–20Ag20CaF₂ composite at 650° C. *Tribology Letters*, 6(3-4), 225-232.
- [68] Doğan, C. P., & Hawk, J. A. (2000). Influence of whisker toughening and microstructure on the wear behavior of Si₃N₄-and Al₂O₃-matrix composites reinforced with SiC. *Journal of materials science*, 35(23), 5793-5807.
- [69] Basavarajappa, S., Chandramohan, G., & Davim, J. P. (2007). Application of Taguchi techniques to study dry sliding wear behaviour of metal matrix composites. *Materials & design*, 28(4), 1393-1398.
- [70] Mahendra, K. V., & Radhakrishna, K. (2007). Fabrication of Al–4.5% Cu alloy with fly ash metal matrix composites and its characterization. *Materials Science-Poland*, 25(1), 57-68.
- [71] Ganesh, V. V., & Chawla, N. (2004). Effect of reinforcement-particle-orientation anisotropy on the tensile and fatigue behavior of metal-matrix composites. *Metallurgical and Materials Transactions A*, 35(1), 53-61.

- [72] Mochida, T., Taya, M., & Lloyd, D. J. (1991). Fracture of particles in a particle/metal matrix composite under plastic straining and its effect on the Young's modulus of the composite. *Materials Transactions, JIM*, 32(10), 931-942.
- [73] Rohatgi, P. K., Ray, S., & Liu, Y. (1992). Tribological properties of metal matrix-graphite particle composites. *International materials reviews*, 37(1), 129-152.
- [74] Melendez, I. M., Neubauer, E., Angerer, P., Danninger, H., & Torralba, J. M. (2011). Influence of nano-reinforcements on the mechanical properties and microstructure of titanium matrix composites. *Composites Science and Technology*, 71(8), 1154-1162.
- [75] Segerström, S., & Ruyter, I. E. (2009). Effect of thermal cycling on flexural properties of carbon–graphite fiber-reinforced polymers. *dental materials*, 25(7), 845-851.
- [76] Kestursatya, M., Kim, J. K., & Rohatgi, P. K. (2003). Wear performance of copper–graphite composite and a leaded copper alloy. *Materials Science and Engineering: A*, 339(1), 150-158.
- [77] Lee, C. J., Huang, J. C., & Hsieh, P. J. (2006). Mg based nano-composites fabricated by friction stir processing. *Scripta Materialia*, 54(7), 1415-1420.
- [78] Sharma, S. C., Girish, B. M., Satish, B. M., & Kamath, R. (1997). Mechanical properties of As-cast and heat-treated ZA-27 alloy/short glass fiber composites. *Journal of materials engineering and performance*, 7(1), 93-99.
- [79] Poddar, P., Mukherjee, S., & Sahoo, K. L. (2009). The microstructure and mechanical properties of SiC reinforced magnesium based composites by rheocasting process. *Journal of materials engineering and performance*, 18(7), 849-855.
- [80] Slutter, R. G., & Driscoll Jr, G. C. (1963). Flexural strength of steel and concrete composite beams.

List of Publications in Conferences

- 1) **Abhisek Pandey**, Shivam Mishra, Amar Patnaik, 2015, Review on graphite reinforced Metal Matrix Composite, National Conference on Futuristic Approaches in Civil & Mechanical Engg, Jaipur
- 2) Shivam Mishra, **Abhisek Pandey**, Amar Patnaik, 2015, Optimization of Reciprocating Wear Performance of Garnet & Graphite reinforced Al7075 alloy hybrid Composite Using Taguchi Method, National Conference on Futuristic Approaches in Civil & Mechanical Engg, Jaipur.
- 3) Shivam Mishra, **Abhisek Pandey**, Amar Patnaik, 2015, Analysis of Tribological behavior of Fly-ash & Graphite reinforced Al7075 alloy under reciprocating motion, International conference on Emerging & Futuristic Trend in Engg and Technology, Chandigarh.
- 4) **Abhisek Pandey**, Shivam Mishra, Amar Patnaik, 2015, A Review on Failure of Ball Bearing under Various Loading Conditions, International conference on Emerging & Futuristic Trend in Engg and Technology, Chandigarh